The relationship between negative BOLD responses and ERS and ERD of alpha/beta oscillations in visual and motor cortex

Ross Wilson[a], Karen J. Mullinger[a,b], Susan T. Francis[b], Stephen D. Mayhew[a]†

[a] Centre for Human Brain Health (CHBH), University of Birmingham, Birmingham, UK

[b] SPMIC, School of Physics and Astronomy, University of Nottingham, Nottingham, UK

† corresponding author

Highlights

EEG-fMRI study of negative BOLD in stimulated and unstimulated sensory cortex

Visual and motor stimuli both induce intra- and cross-modal negative BOLD responses

CM ERS of alpha/beta power inconsistent across subjects, but linked to larger CM NBR

Single-trial EEG-NBR correlations further support neural origin of NBR

Abstract

Previous work has investigated the electrophysiological origins of the intra-modal (within the stimulated sensory cortex) negative BOLD fMRI response (NBR, decrease from baseline) but little attention has been paid to the origin of cross-modal NBRs, those in a different sensory cortex. In the current study we use simultaneous EEG-fMRI recordings to assess the neural correlates of both intra- and cross-modal responses to left-hemifield visual stimuli and right-hand motor tasks, and evaluate the balance of activation and deactivation between the visual and motor systems. Within- and between-subject covariations of EEG and fMRI responses to both tasks are assessed to determine how patterns of event-related desynchronization/synchronisation (ERD/ERS) of alpha/beta frequency oscillations relate to the NBR in the two sensory cortices.

We show that both visual and motor tasks induce intra-modal NBR and cross-modal NBR (e.g. visual stimuli evoked NBRs in both visual and motor cortices). In the EEG data, bilateral intra-modal alpha/beta ERD were consistently observed to both tasks, whilst the cross-modal EEG response varied across subjects between alpha/beta ERD and ERS. Both the mean cross-modal EEG and fMRI response amplitudes showed a small increase in magnitude with increasing task intensity.

In response to the visual stimuli, subjects displaying cross-modal ERS of motor beta power displayed a significantly larger magnitude of cross-modal NBR in motor cortex. However, in contrast to the motor stimuli, larger cross-modal ERD of visual alpha power was associated with larger cross-modal visual NBR. Single-trial correlation analysis provided further evidence of relationship between EEG signals and the NBR, motor cortex beta responses to motor tasks were significantly

negatively correlated with cross-modal visual cortex NBR amplitude, and positively correlated with intra-modal motor cortex PBR.

This study provides a new body of evidence that the coupling between BOLD and low-frequency (alpha/beta) sensory cortex EEG responses extends to cross-modal NBR.

Keywords: EEG-fMRI, negative BOLD, NBR, alpha, ERS, cross-modal

Introduction

Functional magnetic resonance imaging (fMRI) is widely used as the primary method for localising brain function. Such localisation is typically established by measuring the relative changes in blood oxygenation level dependent (BOLD) signal during stimulation or tasks from baseline. The positive BOLD response (PBR), an increase in signal from resting baseline levels, has been shown to relate closely to changes in local field potential activity (LFP) (Heeger, Huk et al. 2000, Logothetis, Pauls et al. 2001), and therefore provide an indirect, non-invasive measurement of increased neuronal activity. Often overlooked however is the decrease in BOLD signal from resting baseline, termed the negative BOLD responses (NBRs). The mechanisms underlying the NBR remain unclear. Although it shares many response properties with the PBR (Shmuel, Yacoub et al. 2002, Klingner, Hasler et al. 2010), studies suggest it may arise from different neurovascular coupling to the PBR (Mullinger, Mayhew et al. 2014) whilst others cite a lack of influence of pre-existing NBR on subsequent PBR as evidence they arise from overlapping, non-parallel pathways rather than superimposed, independent pathways (Klingner, Ebenau et al. 2011). Although debate remains about the exact extent of vascular contributions to NBR (Harel, Lee et al. 2002, Kannurpatti and Biswal 2004, Devor, Tian et al. 2007, Huber, Goense et al. 2014, Puckett, Mathis et al. 2014), recent work has shown that a substantial component of NBR reflects a decrease in neuronal activity (Shmuel, Yacoub et al. 2002, Shmuel, Augath et al. 2006, Pasley, Inglis et al. 2007, Mullinger, Mayhew et al. 2014, Boorman, Harris et al. 2015, Sten, Lundengard et al. 2017). Therefore the NBR represents a promising means of obtaining a functional neuroimaging measure of neuronal inhibition. Despite the common observation of these responses

during a multitude of tasks, a detailed understanding of the neuronal components underlying the origin of the NBR remains incomplete. The motivation of the current study is to address this.

NBRs have been reported during epileptic activity in human cortex (Kobayashi, Bagshaw et al. 2006) and rat hippocampus (Schridde, Khubchandani et al. 2008), as well as localised to the ventricles (Bianciardi, Fukunaga et al. 2011, Bright, Bianciardi et al. 2014) and large veins (Olman, Inati et al. 2007, Puckett, Mathis et al. 2014) likely related to the vascular steal phenomena. The current study investigates sensory cortex NBR elicited in healthy humans by sensory stimuli, this is most likely to have a neural component and therefore be of functional relevance to cognitive brain function.

In this context, NBRs can be elicited in a variety of cortical regions depending on the stimulus paradigm, and either occur within the cortex directly stimulated (intra-modal, IM) or outside of it. NBRs have been shown to occur in the sensory cortex ipsilateral to a unilateral stimulus (IM ipsilateral NBRs) (Allison, Meador et al. 2000, Mullinger, Mayhew et al. 2014), which in the context of somatosensory stimulation have been shown to be diffuse through S1 and not topographically (Tal, Geva et al. 2017). NBRs are also found adjacent to the PBR in the contralateral sensory cortex (IM surround NBRs) (Pasley, Inglis et al. 2007) which hold topographic information related to somatosensory stimulation (Tal, Geva et al. 2017). NBRs have also been shown to occur in a sensory cortex other than that stimulated (cross-modal, CM NBRs), such as NBRs observed in auditory cortex during visual stimulation and vice versa (Laurienti, Burdette et al. 2002, Hairston, Hodges et al. 2008, Mozolic, Joyner

et al. 2008, Ciaramitaro, Chow et al. 2017), in pre- and post-central gyri, SMA and occipital cortex via caloric vestibular stimulation (Klingner, Volk et al. 2013) or in the default mode network (DNM) during sensory stimulation or cognitive tasks (McKiernan, Kaufman et al. 2003, Buckner, Andrews-Hanna et al. 2008).

Many occurrences of NBR are therefore reported and considered as potential markers of deactivated or down-regulated cortex, However, it remains unknown whether IM, CM and DMN NBR share similar or different origins or whether they reflect comparable brain mechanisms. CM NBR have been linked to inhibition of task irrelevant information (Laurienti, Burdette et al. 2002, Hairston, Hodges et al. 2008) but their neural correlates are unstudied compared to IM and DMN NBRs (Shmuel, Augath et al. 2006, Jerbi, Vidal et al. 2010)). Furthermore, it is currently unknown whether these different IM and CM manifestations of the NBR comprise comparable contributions of vascular and neuronal responses to stimulation, if they relate to similar functional processes, or whether the underlying neuronal mechanisms of these signals fundamentally differ. If the NBR is a measure of changes in neuronal activity, rather than an entirely vascular phenomenon, this raises the question of whether these changes correlate to behaviour or subjective perception. Increasing mean IM ipsilateral NBR magnitude in S1, to contralateral sensory stimuli, has been shown to correlate with increasing tactile perceptual thresholds (Kastrup, Baudewig et al. 2008, Schafer, Blankenburg et al. 2012). CM NBR magnitude has been suggested to relate to filtering out unnecessary information with larger auditory NBRs during visual imagery than during visual stimulation (Amedi, Malach et al. 2005). Only the magnitude of IM NBRs has been shown to alter with stimulus intensity in a

manner similar to the PBR (Shmuel, Yacoub et al. 2002, Klingner, Hasler et al. 2010).

To understand the origins of the NBR, corresponding measurements of electrophysiological responses are illuminating. Seminal studies in primates and rats have shown decreases in gamma (>30Hz) LFP activity in IM NBR regions (Shmuel, Augath et al. 2006, Boorman, Kennerley et al. 2010, Boorman, Harris et al. 2015), providing evidence for a neuronal origin of NBRs. However, the neural correlates of CM NBR remain unstudied. EEG oscillations provide a high temporal resolution measure of fluctuations in the synchrony of the underlying neuronal activity. For low frequency EEG measures, alpha (α; 7-13Hz) and beta (β; 13-30Hz), event related synchronisation (ERS, power increase from baseline) is thought to reflect decreased cortical excitability required to regulate sensory processing (Pfurtscheller, Stancak et al. 1996, Klimesch, Sauseng et al. 2007, Mazaheri and Jensen 2010), and event related desynchronisation (ERD, power decrease from baseline) is believed to represent increased excitability and cortical activation (Pfurtscheller, Neuper et al. 1994, Pfurtscheller and Lopes da Silva 2005). Adrian (Adrian 1944) previously observed CM power increases in α oscillations in visual cortex during auditory stimulation, suggesting that α ERS may be an EEG correlate of CM NBR. More recently both IM and CM α ERS has been suggested as a mechanism for attentional suppression of non-stimulated or task-irrelevant regions (Foxe and Snyder 2011). Thought to reflect resources to suppress distraction, such ERS has been observed in occipital α during auditory attention (Fu, Foxe et al. 2001), in somatosensory (Haegens, Luther et al. 2012) and occipital α ipsilateral to the direction of spatial attention (Worden, Foxe et al. 2000, Thut, Nietzel et al. 2006, Rihs, Michel et al.

2007), and in occipito-parietal α ERS during memory retention (Jensen, Gelfand et al. 2002).

Previous work using combined EEG-fMRI in humans (Mullinger, Mayhew et al. 2014) found that increased single-trial IM ipsilateral NBR magnitude in S1 correlated with increased alpha power in somatosensory cortex, linking IM NBR to decreased cortical activity. Further evidence of links between increased alpha power and IM NBR have been observed in visual cortex during photic stimulation (Maggioni, Molteni et al. 2015). In contrast, Yuan et al (Yuan, Perdoni et al. 2011) found only a coupling between alpha power and IM PBR during unilateral hand movements.

In the current study we use multimodal neuroimaging to record EEG signals and MR based BOLD and cerebral blood flow (CBF) reciprocal responses between visual and sensorimotor cortex induced by separate visual and motor tasks. This study aims to address three questions, to determine 1) whether CM NBR is elicited by motor tasks and visual stimuli, and whether CM and IM NBR are both modulated by task/stimulus intensity; 2) whether there are intrinsic relationships between the magnitudes of (i) IM NBRs and CM NBRs (ii) IM and CM EEG responses; and 3) whether IM and CM NBR are related to IM and CM α/β EEG responses.

We hypothesised that 1) CM NBR would be elicited by motor tasks and visual stimuli with both modulated by stimulus intensity; 2) a. IM NBRs and CM NBRs would be positively correlated; 2) b. IM and CM EEG responses would be negatively correlated; 3) Negative correlations would be found between NBR and α/β EEG responses.

Methods

17 healthy subjects (7 female; mean age 30.6 ±5; all right handed - tested using the Edinburgh handedness inventory, group mean laterality index +96.8±5) gave informed consent to take part. The University of Birmingham ethics committee approved the procedures.

Paradigm

Four separate experimental runs of simultaneous BOLD-CBF-EEG data were recorded. In each run, subjects performed one of two motor tasks of different complexity and two visual tasks of different intensities to modulate BOLD response magnitude. Subjects were instructed to fixate their eyes throughout on a central cross-hair.

The visual stimuli comprised left-hemifield black-white checkerboards of either 100% (High) or 10% (Low) contrast with pattern reversal at 3Hz. This stimulation frequency was chosen to maintain robust fMRI responses whilst minimising contamination of alpha frequency EEG oscillations with stimulus-evoked responses.

Two motor tasks, either a “complex” Tap or a “simple” Grip Motor task, were performed using the right hand. The Tap task (Tap) involved a paired finger-thumb opposition, sequentially tapping each finger to the opposing thumb from index finger to little finger, reversing and repeating. For the Grip task (Grip), a small, easily deformable rubber ball was repeatedly squeezed between the fingers and thumb in a rhythmic manner. Motor tasks, performed at approximately 2Hz, were initiated by a

visual cue of the word “Grip” or “Tap” which was sustained throughout the stimulation period. Instructions were given prior to testing for both tasks and all subjects underwent a ten-minute period of familiarisation with the Tap and the High visual stimuli outside of the scanner.

Our task choice was motivated by previous literature. It is well known that increasing visual contrast increases both fMRI and EEG response magnitude (Singh, Kim et al. 2003, Mayhew, Ostwald et al. 2013). Similarly, in the motor domain, increased recruitment of motor cortex regions have been shown between a simple grip and a more complex finger thumb opposition tasks (Kuhtz-Buschbeck, Mahnkopf et al. 2003). We hypothesized that this increase in PBR with task complexity would be accompanied by a similar increase in NBR and EEG response magnitude. Therefore the motor task conditions were chosen for similar reasons to the two visual contrast levels, to induce a modulation of the fMRI and EEG responses (e.g. we expected larger magnitude responses to Tap than Grip) and to facilitate studying relationships between them.

Each of the four runs started with a 60 second rest period (fixation) to measure the baseline fMRI signal. This was followed by 24 pseudo-randomly ordered trials of High, and Low, and either Tap or Grip. All trials consisted of 14s of stimulation followed by 20s resting-fixation. Of the 24 trials per run, 12 were motor tasks, 6 were High and 6 Low with either Tap or Grip performed in a single run, never both. The order of runs was counterbalanced between subjects. Performance was monitored visually through the video monitor of the scanner bore and also through the console

room window to ensure that subjects accurately performed the motor tasks as instructed.

EEG Data

EEG data was recorded at 5 kHz using a 64 channel MR-compatible EasyCap following the extended international 10-20 system layout. An electrocardiogram (ECG) channel was also attached just below the subject's clavicle. Electrode AFz was used as the ground and FCz used as the reference electrode. All electrode impedances were maintained below 20 kΩ. Data were acquired using BrainAmp MR-plus amplifiers (Brain Products, Munich) and Brain Vision Recorder (Version 1.10).

Gradient artefacts were minimised by positioning the subject such that FP1 and FP2 were at the iso-centre of the scanner's static field whilst equipment related artefacts were minimized by isolating the EEG amplifiers from the scanner bed and ensuring the cryopumps were switched off during acquisition (Mullinger and Bowtell 2011). For consistent waveform sampling, EEG and MR scanner clocks were synchronised and the MRI data volume repetition time (TR) made a multiple of the EEG sampling period (Mandelkow, Halder et al. 2006, Mullinger, Morgan et al. 2008). A Polhemus fastrak 3D system (Polhemus, Vermont, USA) was used to digitize electrode positions for co-registration to the subjects T_1-weighted anatomical scan.

fMRI Data

FMRI data were acquired on a Philips Achieva 3T MR scanner (Philips Medical Systems, Best, Netherlands) using a whole body transmit and a 32-channel head receive coil.

First a 5-minute BOLD localiser scan comprising High and Tap trials was performed. IViewBOLD (Philips real-time processing of fMRI data) was used to statistically map responses in the primary motor (M1) and visual (V1) cortex. A double acquisition background suppressed (DABS) FAIR sequence was then used to acquire both BOLD and arterial spin labelling (ASL) data simultaneously during EEG collection (Mullinger, Cherukara et al. 2017). The localiser was used to plan the 12 oblique-axial slices (voxel size 3.25x3.25x5mm, 212mm FOV, SENSE factor 2.3) to ensure coverage of both motor and visual regions. The DABS sequence comprised a TR=2.6, echo time (TE)=9ms ASL data/TE=40ms BOLD data, post-label delay 1400ms, with background suppression pulses at T_{BGS1}/T_{BGS2} = 339ms / 899ms, with 174 volumes [tag-control pairs] collected per run. Between runs two and three, a 5-minute resting-state DABS scan was also acquired during which subjects were asked to keep their eyes open and centrally fixate. At the end of the scan session a local T_1 anatomical image, and a whole-head T_1-weighted anatomical image (1mm isotropic spatial resolution) were acquired to aid co-registration.

Throughout all scans, the vector cardiogram (VCG) and respiratory bellows were used to record cardiac and respiratory cycles respectively.

Pre-processing and Analysis

EEG DATA

EEG data were pre-processed in Brain Vision Analyser 2. Heart beat events were detected from the VCG trace and used to mark cardiac cycles in the EEG data. MR gradient and pulse artefact correction was performed using sliding template average-artefact subtraction (21 events per template for both artefacts) (Allen, Josephs et al. 2000, Mullinger, Cherukara et al. 2017). The data were filtered between 1-70 Hz and then downsampled to 600 Hz. Noisy trials/channels were found via visual inspection and excluded from further analysis and data re-referenced to an average of all non-noisy channels. Data were exported to the Fieldtrip open source Matlab toolbox (http://www.ru.nl/fcdonders/fieldtrip (Oostenveld, Fries et al. 2011)) and then band-pass filtered into α (7-13Hz) and β (13-30 Hz) frequency datasets for source analysis.

EEG Beamforming

Sources of α and β responses to visual and motor tasks were reconstructed using a linearly constrained minimum variance (LCMV) beamformer (Van Veen 1997) implemented in FieldTrip. Digitized EEG electrode positions were co-registered with the subjects' T_1-weighted image. A 4-shell, anatomically realistic volume conduction boundary element model (BEM), was created by segmenting each subject's T_1-weighted anatomical into skin, skull, cerebrospinal fluid and brain compartments. A template grid (5mm spacing) was created from the MNI brain and transformed to each subject's anatomical space. The leadfield matrix at each location on the template grid in individual subject space was then calculated using their BEM.

The LCMV beamformer analyses were carried out for each subject using: i) all visual data combined and ii) all motor data combined. This combination of data over stimulus intensities was carried out because, as expected, preliminary analysis showed comparable spatial response locations between conditions of the same stimulus modality, and the accuracy of beamforming is increased by increasing the amount of data (Brookes, Mullinger et al. 2008). Separately for each task, and for both α and β frequency bands, the LCMV beamformer with a regularization parameter of 0.01% was used to calculate a spatial filter (weights of each EEG channel at each leadfield grid position) using the full timecourse of all relevant trials (0-34seconds). These weights were then used to calculate the source power for each position in the template grid during the stimulus period (0.5-13.5s) and, separately for a matching duration at the end of the baseline period (20.5-33.5s). A contrast was calculated between the source power of the stimulus period and baseline: (stimulus-baseline)/baseline (Robinson and Vrba 1999) to generate a power ratio map to localize both ERD (stimulus power lower than baseline) and ERS (stimulus power higher than baseline) in response to the stimuli. From these maps virtual electrode (VE) positions of peak ERD power change in motor and visual cortex were separately located for each subject. The maximum α ERD was located in visual cortex to all visual trials combined (vVE) and the maximum β ERD in the motor cortex to all motor trials combined (mVE). The use of one spatial location per sensory cortex enabled the assessment of CM EEG responses using an independently selected region of interest, assuming no spatial difference between IM and CM responses. Given the limited spatial resolution of EEG, this assumption is reasonable and subsequent visual inspection of single-subject beamformer maps

confirmed that no CM responses occurred consistently in other regions of sensory cortex

Timecourses of α and β neural activity were extracted from the vVE and mVE for each run and the absolute value of the Hilbert transform used to obtain the oscillatory power timecourse. VEs were then epoched into single-trials for each stimulus condition: Grip, Tap, High and Low. For each VE, each subject's data was normalized to a zero amplitude baseline by subtraction of their passive period (20.5-33.5s) mean amplitude. Separately for both α and β frequency bands, the IM and CM single-trial response amplitudes were then calculated from the respective VEs as the mean VE amplitude during the stimulus window (0.5-13.5s). For each subject the IM and CM responses were classified as either ERD or ERS depending on whether their mean stimulus power showed lower or higher power than the passive period respectively. Group IM and CM responses were tested for significance from baseline (student's t-test vs zero amplitude). The following within- and between-subject correlations of response amplitudes were then calculated: between frequency bands (e.g. Low α vs Low β); between brain regions (e.g. Low IM vs Low CM) and between conditions (Low α vs High α). Subsequently, due to the high degree of similarity found between EEG α and β response amplitudes (see Results section), β data were used as summary measures of the motor cortex response to tasks (IM motor and CM visual) while α data were used as summary measures of the visual cortex response to tasks (IM visual and CM motor). For brevity and to minimise the number of tests performed we omit reporting both α and β responses for each task. In addition, whilst some studies conflate the two, α and β oscillations are separate, distinct neural signals, with only weakly related spontaneous activity (Carlqvist,

Nikulin et al. 2005), and understanding of their origins and generative mechanisms remains incomplete. Furthermore, some recent work suggests independent roles of alpha and beta in motor actions (Brinkman, Stolk et al. 2014, Brinkman, Stolk et al. 2016) we therefore chose to preserve consistency in analysis approach between visual and motor tasks and specificity to individual frequency bands, in line with other recent EEG-fMRI studies (Ritter, Moosmann et al. 2009, Yuan, Liu et al. 2010).

Finally, separately for both the IM and CM responses, the trial-by-trial power during the stimulus period was mean-subtracted and used to form parametric modulation regressors for the fMRI general linear modelling (GLM) analysis to localise fMRI responses that correlated with this neuronal activity. These analyses were used to test question 3 posed above – whether IM/CM EEG responses were related to the IM /CM NBRs.

fMRI Data

BOLD and ASL data were separated from the DABS output. RETROICOR (Glover, Li et al. 2000) was used to correct the BOLD data for physiological noise. Physiological noise correction is unnecessary for ASL data since it is background suppressed with a short TE: nulling the tissue magnetisation signal to zero leads to a reduction in physiological noise (Garcia, Duhamel et al. 2005). Data were motion corrected using MCFLIRT (Jenkinson and Smith 2001, Jenkinson, Bannister et al. 2002) (FSL, http://www.fmrib.ox.ac.uk/fsl/) and interpolated to an effective TR of 2.6. Perfusion-weighted CBF images were formed by subtracting tag from control ASL image pairs, BOLD image pairs were averaged creating mean BOLD-weighted data. BOLD data were normalised to the standard MNI template using FLIRT and the

same transform was then applied to the ASL data. Further pre-processing was carried out in FSL. Data were spatially smoothed with a Gaussian kernel (5 mm FWHM) and temporally filtered (high pass cut-off >0.01Hz).

Two subject's data were removed from further analysis due to a large number of head movement artefacts >4mm, as identified from realignment parameters.

fMRI Statistical analysis

Separate GLM analyses of BOLD and ASL data were carried out using FEAT v6.0 in FSL. Design matrices consisted of six regressors per run, the main effect of each motor (tap or grip) and visual (high and low) condition was modelled using a constant amplitude boxcar regressor along with the corresponding stimulus-period EEG power regressor described above. Two separate GLMs were formed for each run, incorporating either the IM or CM EEG power regressor: IM (motor = mVE β, visual= vVE α) and CM (motor = vVE α, visual = mVE β).

All regressors were convolved with a double-gamma haemodynamic response function (HRF). Both positive and negative Z-contrasts (cluster corrected $z>2.0$, $p<0.05$) were computed for each regressor. Subject average responses across all runs were calculated at the second-level using fixed effects and then group average maps were calculated across subjects using mixed effects FLAME 1+2 (Woolrich, Behrens et al. 2004) cluster corrected ($p<0.05$).

Region of Interest (ROI) Analysis

A motor cortex (M1) mask and a visual cortex (V1) mask were created from the Harvard-Oxford Cortical Structural Atlas (Desikan, Ségonne et al. 2006). Regions of interest of 1.5 radius (27 voxel) spheres, were generated centred upon voxels with highest second level main effect BOLD statistical significance within the relevant sensory mask region. ROIs defined were in: 1) contralateral M1 for the IM motor PBRs and CM visual NBR; 2) ipsilateral M1 for IM motor NBRs; 3) contralateral V1 for IM visual PBRs; 4) ipsilateral V1 for IM visual NBRs; 5) Left superior LOC for CM motor NBRs. The average ROI BOLD responses to each stimulus were then extracted from each ROI, from the preprocessed data. The mean percentage signal change of the BOLD response was calculated relative to baseline, which was taken as the first 60 seconds of the entire run to provide the most representative baseline. These mean BOLD responses were then used to investigate relationships between IM and CM responses by calculating IM PBR versus CM NBR, and IM NBR versus CM NBR.

Pearson's linear correlations were then carried out between the IM PBR and IM NBR, IM PBR and CM NBR, and the IM NBR and CM NBR.

Results

fMRI group main effect to motor and visual stimuli: *Question 1*

The main effect GLMs showed both NBRs and PBRs were induced in IM and CM cortices to motor (Figure 1) and visual (Figure 2) stimuli, with corresponding negative CBF (NCBF) and positive CBF (PCBF) responses. Table 1 and Table 2 compare the spatial extent and statistical significance of NBRs and PBRs between tasks and the spatial conjunction between BOLD and CBF responses for IM and CM fMRI responses respectively. As only IM ipsilateral NBRs, and not IM surround NBRs,

were observed in this data we simply refer to IM ipsilateral NBRs as IM NBRs unless otherwise stated.

Motor Stimuli

Intra-modal (IM) responses

The IM NBR and NCBF evoked by both motor tasks were located in ipsilateral (left) and medial M1, the cingulate cortex and bilateral frontal regions (Figure 1D&E). The contrast *Tap > Grip* showed that the Tap IM NBR was significantly larger than Grip IM NBR (Figure 1F; Tap/Grip: 884/ 564 voxels, see Table 1), with a higher NBR peak Z-stat (Tap/Grip: Z=4.6/4.3); locations specified in Table 1). Both Tap and Grip showed good spatial correspondence of IM NBR and IM NCBF responses as shown by the size of their conjunction (Tap: 21%, Grip: 8%; see Table 1).

The IM PBR and PCBF were observed in contralateral (right) M1 (Figure 1D&E) with considerable spatial overlap with PCBF responses (Tap/Grip: 72%/65%, see Table 1). No statistically significant voxel-wise differences were evident between Grip and Tap IM PBRs (Figure 1F).

Cross-modal (CM) responses

The CM NBR and NCBF evoked by the motor tasks were observed in widespread areas of visual cortex including V1, cuneal cortex, and the lateral occipital cortex (LOC) in bilateral regions for the Tap task, whilst mostly contralateral for the Grip task (Figure 1A&B). Both CM NBR and NCBF were significantly larger in magnitude during Tap than Grip (Figure 1C). The Tap task evoked CM NBR with much greater spatial extent (Tap/Grip: 5452/859 voxels, see Table 2), peak BOLD Z-stat (Tap/Grip: Z=4.8/3.9, locations specified in Table 2), and CM NBR/NCBF overlap

(Tap/Grip: 45%/24%, see Table 2) than the Grip task. In addition, CM PBRs were also evoked by both Grip and Tap tasks in bilateral inferior LOC located inferior to the CM NBRs (Figure 1A&B).

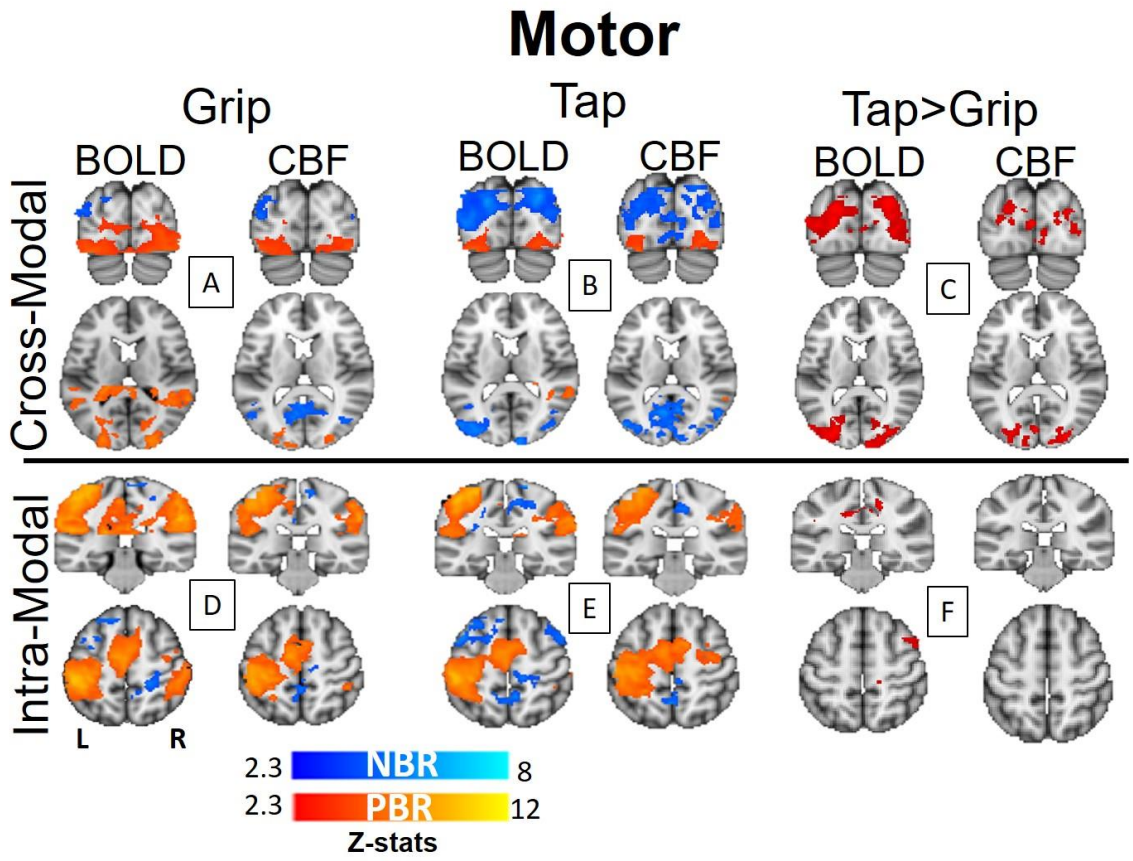

Figure 1. BOLD and CBF response to motor task.
A and D show the main effect BOLD and CBF responses to Grip in the CM (top panel) and IM (bottom panel) cortices respectively. B and E show the main effect BOLD and CBF responses to Tap in the CM and IM cortices respectively. C and F show the contrast (Tap>Grip) highlighting the CM (F) and IM (C) regions which are more significant in Tap than Grip respectively. Blue=NBR, red=PBR. Motor cortex (IM) y=48, z=63. Visual cortex (CM) y=22, z=42.

Visual Stimuli

Intra-modal (IM) responses

The NBR and NCBF evoked by High and Low contrast visual stimuli were located in ipsilateral V1, with responses extending bilaterally in anterior V1. High contrast visual stimuli also evoked IM NBR bilaterally in LOC and the intraparietal lobe (IPL) (Figure

2A&B). Both High and Low contrast showed good spatial correspondence between IM NBR and IM NCBF responses as shown by the size of their conjunction (High/Low: 21%/46%, see Table 1). The *High>Low* stimuli showed significantly larger magnitude NBR in more dorsal areas such as the precuneus and bilateral LOC for the High contrast compared to Low (Figure. 2C), with a larger NBR peak Z-stat (High/Low: Z=5.0/3.6, see Table 1).

Peak IM PBR and PCBF to both the High and Low stimuli were located in contralateral V1 (Figure. 2A&B) with high levels of spatial overlap (High: 68%, Low: 70%, see Table 1). PBR and PCBF response amplitudes and extent were very similar between High and Low stimuli (Figure. 2C and Table 1).

Cross-modal (CM) responses

CM NBR and NCBF to High visual stimuli were located in bilateral M1 (stronger contralateral to the stimulus), bilateral secondary sensorimotor cortex and supplementary motor area (SMA) (Figure 2E) (peak Z=4.09, extent 1634, NBR/NCBF overlap 52%, see Table 2). There was considerable spatial overlap between the location of the High CM NBR and the motor IM PBR in left M1 and SMA (spatial overlap: High CM NBR and IM Tap PBR 1265 voxels; High CM NBR and IM Grip PBR 1391 voxels). No significant CM NBR was observed to Low visual stimuli (Figure 2D, Table 2), but there was no significant difference in NBR for *High >Low* (Figure 2F). In addition, CM PBR was observed in regions bordering the motor cortices (Figure 2D&E), but with no significant difference for *High > Low* stimuli.

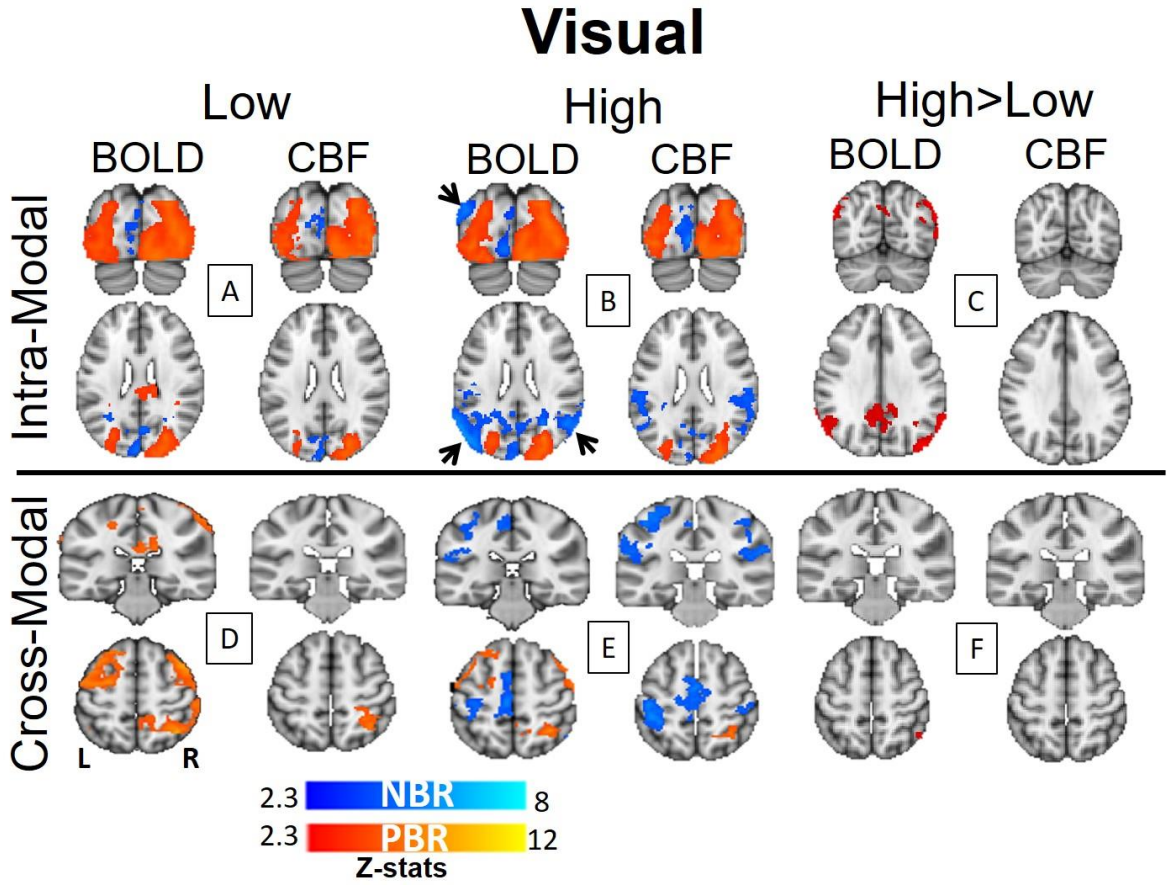

Figure 2. BOLD and CBF response to visual trials.
A and D show the main effect BOLD and CBF responses to Low in the CM (bottom panel) and IM (top panel) cortices respectively. B and E show the main effect BOLD and CBF responses to High in the CM and IM cortices respectively. Arrows highlight High NBRs located in the LOC. C and F show the contrast between High and Low highlighting the CM (F) and IM (C) regions which are more significant in Tap than Grip respectively. Blue=NBR, red=PBR; black arrows show position of lateral occipital cortex NBR. For A,B,D and E: Visual cortex (IM) y=22, z=48, Motor cortex (CM) y=48, z=63. For C and F: Visual cortex (IM) y=30, z=52, Motor cortex (CM) y=48, z=63.

					Peak voxel coordinate		
Task	Response	Spatial extent (voxels)	% overlap with BOLD	Peak BOLD Z-stat	X	Y	Z
Visual (V1)							
High	PBR	8361	68	6.1	38	20	27
High	PCBF	6227					
High	NBR	3563	21	5.0	67	22	50
High	NCBF	1919					
Low	PBR	8668	70	5.9	38	18	30
Low	PCBF	6627					
Low	NBR	1623	46	3.6	47	18	42
Low	NCBF	1124					
Motor (M1)							
Tap	PBR	6018	72	5.2	68	46	64
Tap	PCBF	5997					
Tap	NBR	884	21	4.6	43	38	64
Tap	NCBF	426					
Grip	PBR	6956	65	6.0	63	45	68
Grip	PCBF	5585					
Grip	NBR	564	8	4.3	35	44	68
Grip	NCBF	294					

Table 1. Summary of group level IM responses for visual and motor tasks. Spatial extent was calculated as number of voxels Z>2.0 within the bilateral IM mask. The percentage overlap is the conjunction of significant BOLD and CBF voxels (Z>2.0). The peak response coordinate is taken from the BOLD peak voxel. Peak voxels and percentage overlap are from the contralateral (positive responses) and ipsilateral (negative responses) IM mask respectively.

					Peak voxel coordinate		
Task	Response	Spatial extent (voxels)	% overlap with BOLD	Peak BOLD Z-stat	X	Y	Z
Motor (M1)							
High	PBR	1836	1	4. 1	41	70	72
High	PCBF	63					
High	NBR	1634	52	4.1	48	52	61
High	NCBF	4168					
Low	PBR	4051	2	4.4	66	61	66
Low	PCBF	245					
Low	NBR	-	-	-	-	-	-
Low	NCBF	-					
Visual (V1)							
Tap	PBR	3176	42	5.4	63	21	26
Tap	PCBF	1726					
Tap	NBR	5452	45	4.8	31	23	51
Tap	NCBF	7058					
Grip	PBR	11075	29	5.7	61	20	27
Grip	PCBF	3637					
Grip	NBR	859	24	3.9	66	20	46
Grip	NCBF	2115					

Table 2. Summary of group-level CM peak responses for visual and motor tasks.
The spatial extent was calculated as the number of voxels Z>2.0 within the bilateral CM mask. The peak response coordinate is taken from the BOLD peak voxel. The percentage overlap is the conjunction of significant BOLD and CBF voxels.

Spatial relationship between IM and CM NBRs: Question 2a

The Tap CM NBR was found to overlap with High IM NBR (453 voxels) in left LOC and left V1 and with Low IM NBR (171 voxels) in left V1 (compare Figs 1B with 2A&B). The Tap CM NBR also overlapped with High IM PBR (2125 voxels) and Low IM PBR (2302 voxels) bilaterally in the LOC. Grip CM NBR overlapped with High IM NBR (261 voxels) in left LOC and left V1 as well as with Low IM NBR (21 voxels) in left V1 (compare Figs 1A with 2A&B). Grip CM NBR overlapped with the High IM PBR (58 voxels) and with Low IM PBR (82 voxels) in the left LOC. The High CM NBR did not overlap with the Tap or Grip IM NBR.

We also investigated relationships between sensory cortex BOLD responses to the same task by correlating subjects' CM NBR amplitude with their IM PBR or IM NBR amplitude for each task condition, there were no significant relationships between IM PBR and CM NBRs, although a positive trend ($r=0.51$, $p=0.049$) was seen for the Tap data, Figure S1. However, we did find evidence of a significant positive correlation between subject's IM NBR and CM NBR to both motor tasks (Tap/Grip: $r=0.73/0.68$, both $p<0.01$, Figure S2). No correlations were observed for the visual data between subjects' IM and CM NBRs.

EEG Responses

Figure 3 displays group mean source beamformer maps calculated on the MNI template grid, Fig. 3A and B show the beta response to motor trials and alpha response to visual trials respectively, whilst Fig. 3C and D show group level beamformer maps of alpha response to motor trials and beta response to visual trials.

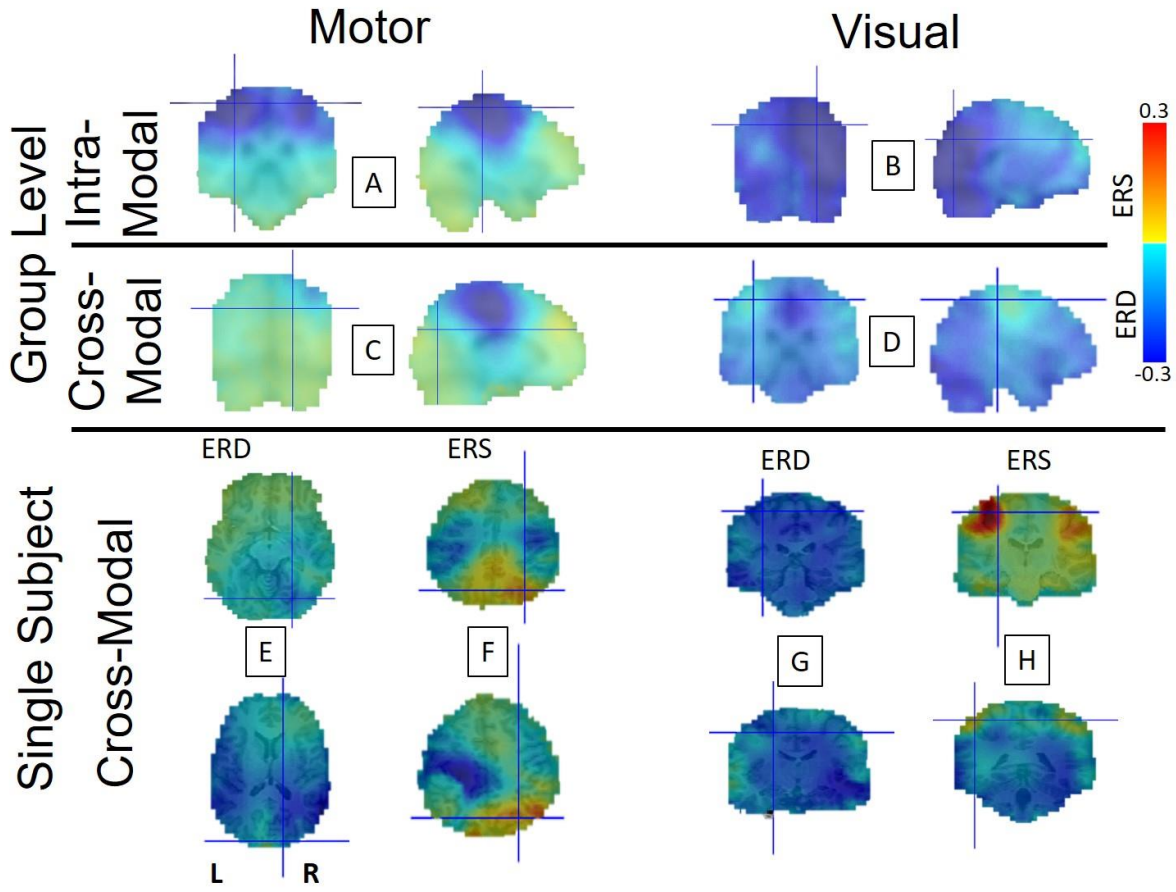

Figure. 3 EEG beamformer maps.
A and **B** show group level beamformer maps of beta response to motor trials and alpha response to visual trials respectively; with the maximum IM ERD related to each modality highlighted by the crosshair. **C** and **D** show group level beamformer maps of alpha response to motor trials (C), and beta response to visual trials (D), the crosshair centred on the other modalities peak ERD response. **E** shows two subjects which present with CM ERD in the vVE *to motor trials*. **F** shows two subjects which present with CM ERS in the vVE to the same *motor trials*. **G** shows two subjects which present with CM ERD in the mVE *to visual trials*. **H** shows two subjects which present with CM ERS in the mVE *to the same visual trials*. Heat maps: red = greater ERS, Blue=greater ERD.

***Motor Trials**: Intra-Modal responses*

Figure 4 displays the group timecourses taken from the mVE location showing a clear group α and β power ERD during the stimulus period for both the Grip and Tap

trials. In all subjects, the peak IM motor ERD, defining the mVE location, was located in contralateral M1, with all subjects showing bilateral IM ERD (see Fig 3A).

Across subjects, the amplitude of the ERD was found to be significantly lower than baseline for both α (Tap = -29.3 ± 20.3nAm, $p<0.001$; Grip = -20.3 ± 19.1nAm, $p<0.01$; p values via one-sample t-test) and β (Tap = -22.5 ± 11.7nAm, $p<0.001$; Grip = -18.3 ± 10.4nAm, $p<0.001$) frequency oscillations (Figure 4A-D). Significantly larger magnitude ERD were observed in response to Tap than to Grip for α (Figure 4E) and β (Figure 4F) power (paired t-test α: $p<0.05$; β: $p<0.05$). α ERD and β ERD showed similar magnitudes, with no significant difference between them for either Tap ($p=0.05$, paired t-test), or Grip ($p=0.62$) (Figure 4G&H respectively). All Tap and Grip task responses showed a rebound of oscillatory power occurring approximately 0-10s after stimulus cessation, whose amplitude was larger in the β than α band.

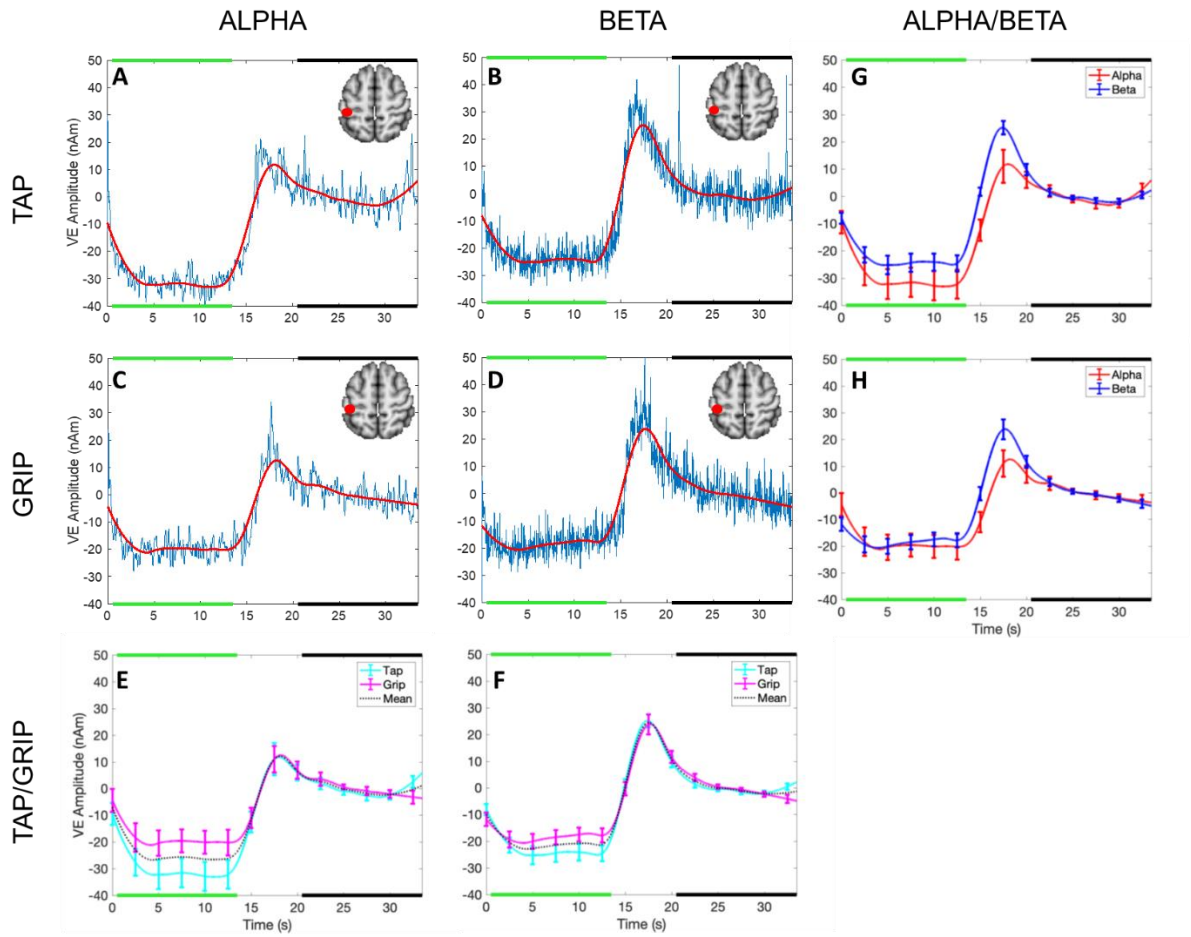

Figure 4. Group average IM motor EEG alpha and beta power timecourses from the mVE.
A and **B** show Tap alpha and beta timecourses respectively (blue= group average raw power timecourse, red=smoothed timecourse). **C** and **D** show Grip alpha and beta timecourses respectively. **E** shows the comparison of Tap and Grip alpha responses (cyan/magenta = Tap/Grip smoothed timecourse, respectively); whilst **F** displays the same for beta responses. Error bars denote the standard deviation across subjects. **G** displays the smoothed timecourses of Tap alpha (red) and beta (blue) responses; whilst **H** shows the same for Grip. Stimulus onset at 0 s, 14 s duration (0.5-13.5s used for analysis: green line). Baseline period 20.5-33.5 seconds (black line). Insert of axial brain slices show general region timecourses were extracted from (mVE).

***Motor Trials**: Cross modal responses*

The group level vVE responses to the motor tasks showed no-significant change between the stimulus period and baseline (Fig 5, α power: Tap = -1.5 ± 9.7nAm, p=

0.57; Grip = -4.0 ± 13.8nAm, p=0.28 [p value via one-sample t-test]; β power: Tap = 0.5 ± 5.2nAm, p=0.68; Grip = -0.1 ± 5.1nAm, p=0.92). However, despite minimal mean stimulus response, both α and β CM motor responses showed a rebound in power between 0-10s post-stimulus.

No significant difference was found between Grip and Tap responses for α (p =0.26; Figure 5E) or β (p=0.64; Figure 5F) frequencies; or between α and β power during either Tap (p=0.33, paired t-test) or Grip (p=0.19), Figure 5G&H. The group motor CM timecourses exhibited a short transient (~500ms) decrease in α and β power at the stimulus onset, and also at offset for β (Figure 5A-D). These transient decreases in power likely represent onset and offset responses related to the presentation of the word ‘Grip’ or ‘Tap’ at the start of the trial and its removal at the end of the trial.

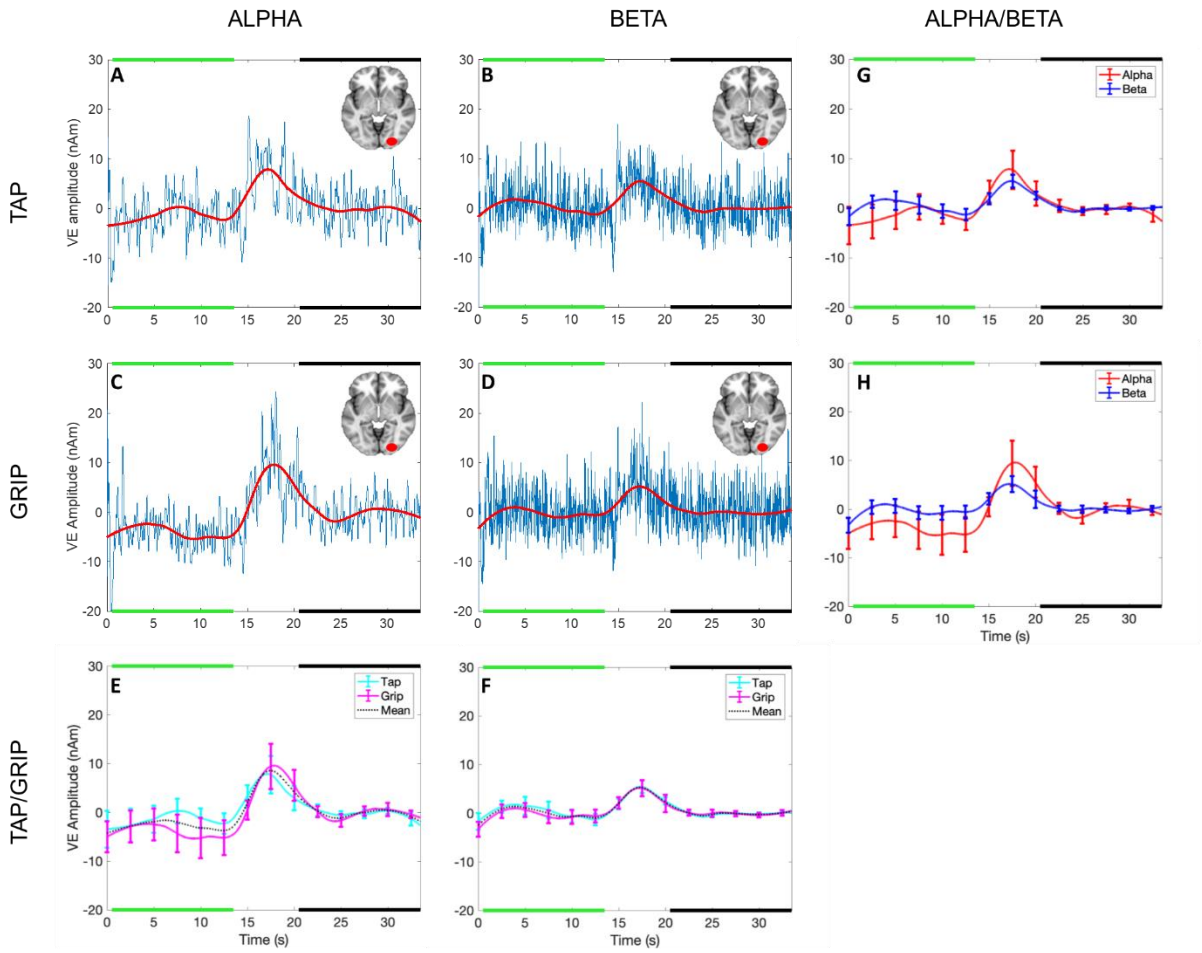

Figure 5. Group average CM motor EEG alpha and beta power timecourses, taken from the vVE.

A and **B** show Tap alpha and beta group average timecourses respectively (blue= group average raw power timecourse, red=smoothed timecourse). **C** and **D** show Grip alpha and beta timecourses respectively. **E** shows the comparison of Tap and Grip alpha responses (cyan/magenta = Tap/Grip smoothed timecourse, respectively); whilst **F** displays the same for beta responses. Error bars denote the standard deviation across subjects. **G** displays the smoothed timecourses of Tap alpha (red) and beta (blue) responses; whilst **H** shows the same for Grip. Stimulus onset at 0 s, 14 s duration (0.5-13.5s used for analysis: green line). Baseline period 20.5-33.5 seconds (black line). Insert of axial brain slices show general region timecourses were extracted from (vVE).

***Visual Trials**: Intra modal responses*

Figure 6 displays the timecourses taken from the vVE location showing group level α and β power ERD throughout the stimulus period for both High and Low trials.

The peak IM visual ERD, defining the vVE location, was located in contralateral V1 in 10 subjects, and in central V1 in 4 subjects. The amplitude of the ERD was significantly lower than baseline for both α (High = -15.7 ± 11.6nAm, $p<0.001$; Low = -15.9 ± 14.6nAm, $p<0.001$) and β (High = -5.4 ± 4.8nAm, $p<0.001$; Low = -7.4 ± 4.1nAm, $p<0.001$) frequency oscillations (Figure 6A-D). High and Low contrast stimuli showed similar α ERD (paired t-test: $p=0.93$, Figure 6E), while the Low contrast showed significantly larger magnitude β ERD than High contrast trials ($p=0.04$, Figure 6F). Significantly larger magnitude α ERD than β ERD was observed during both High (paired t-test: $p<0.01$) and Low ($p<0.05$) trials, Figure 6G&H. All responses showed a rebound of oscillatory power between 0-10s after stimulus cessation, which had larger amplitude for α than β frequencies.

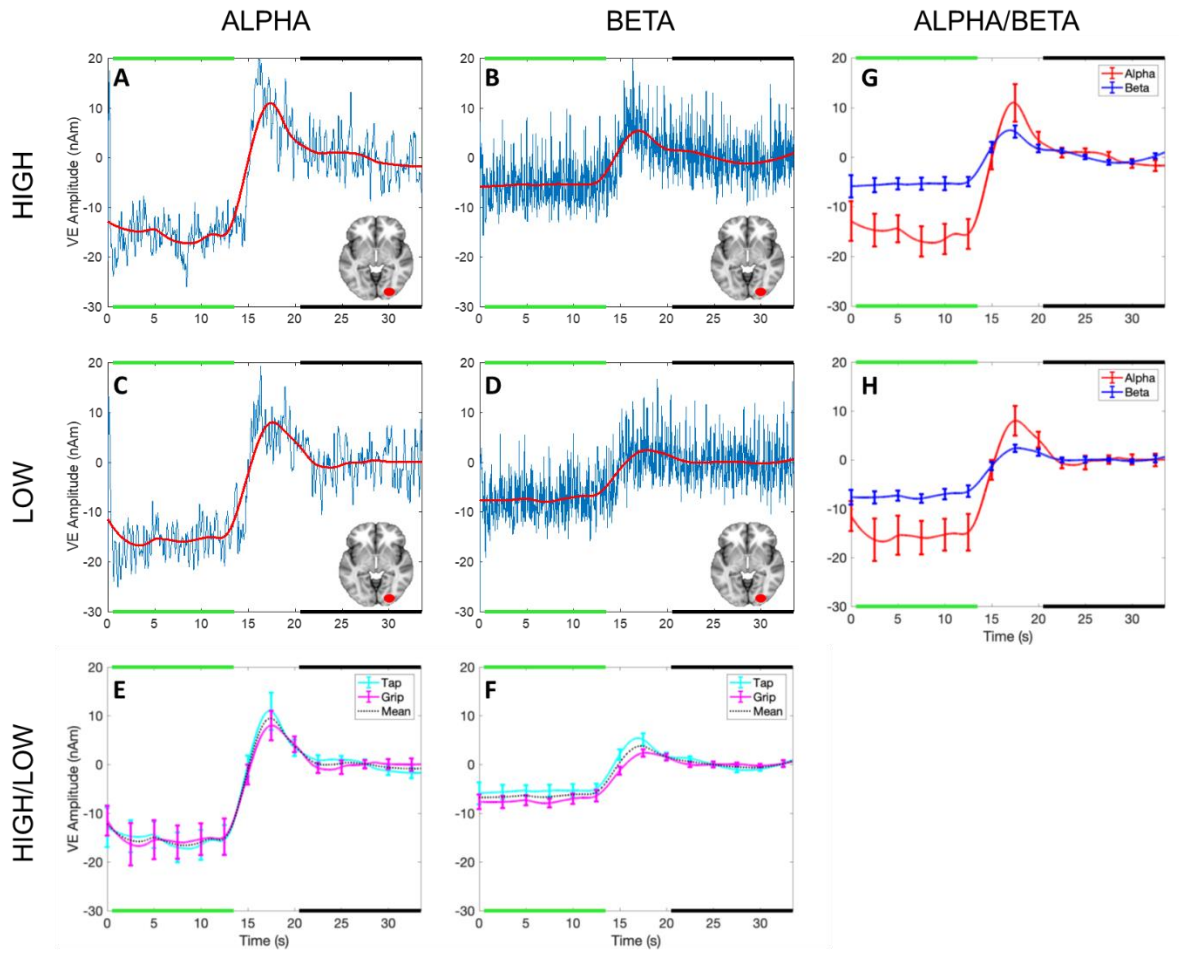

Figure 6. Group average IM visual EEG alpha and beta power timecourses, taken from the vVE.
A and **B** show High alpha and beta timecourses respectively (blue= group average raw power timecourse, red=smoothed timecourse). **C** and **D** show Low alpha and beta timecourses respectively. **E** shows the comparison of High and Low alpha responses (cyan/magenta = High/Low smoothed timecourse, respectively); whilst **F** displays the same for beta responses. Error bars denote the standard deviation across subjects. **G** displays the smoothed timecourses of High alpha (red) and beta (blue) responses; whilst **H** shows the same for Low. Stimulus onset at 0 s, 14 s duration (0.5-13.5s used for analysis: green line). Baseline period 20.5-33.5 seconds (black line). Insert of axial brain slices show general region timecourses were extracted from (vVE).

***Visual Trials**: Cross modal responses*

The group level mVE responses to the visual stimuli showed that Low visual stimuli induced a small but significant CM ERD in motor cortex α power (Figure 7C) (ERD =

-3.6±6.3nAm, $p<0.05$), but no significant change in α power was seen during High trials (Figure 7A; ERD= -1.4±6.5nAm, $p=0.41$), despite similar α responses between High and Low (Figure 7E; paired t-test: $p=0.21$). No significant CM β response was observed for either stimulus (Figure 7B&D; High: ERD= -1.1±4.7nAm, $p=0.38$; Low: ERD= -2.7±5.7nAm, $p=0.09$), with similar CM β power observed between intensities (Fig 7F, $p=0.32$). Similarly no significant difference between α and β frequencies for either High (Figure 7G; paired t-test: $p=0.74$) or Low (Figure 7H; $p=0.35$) was found. All CM visual responses showed a rebound of oscillatory power between 0-10s after stimulus cessation, with larger amplitude for High than Low.

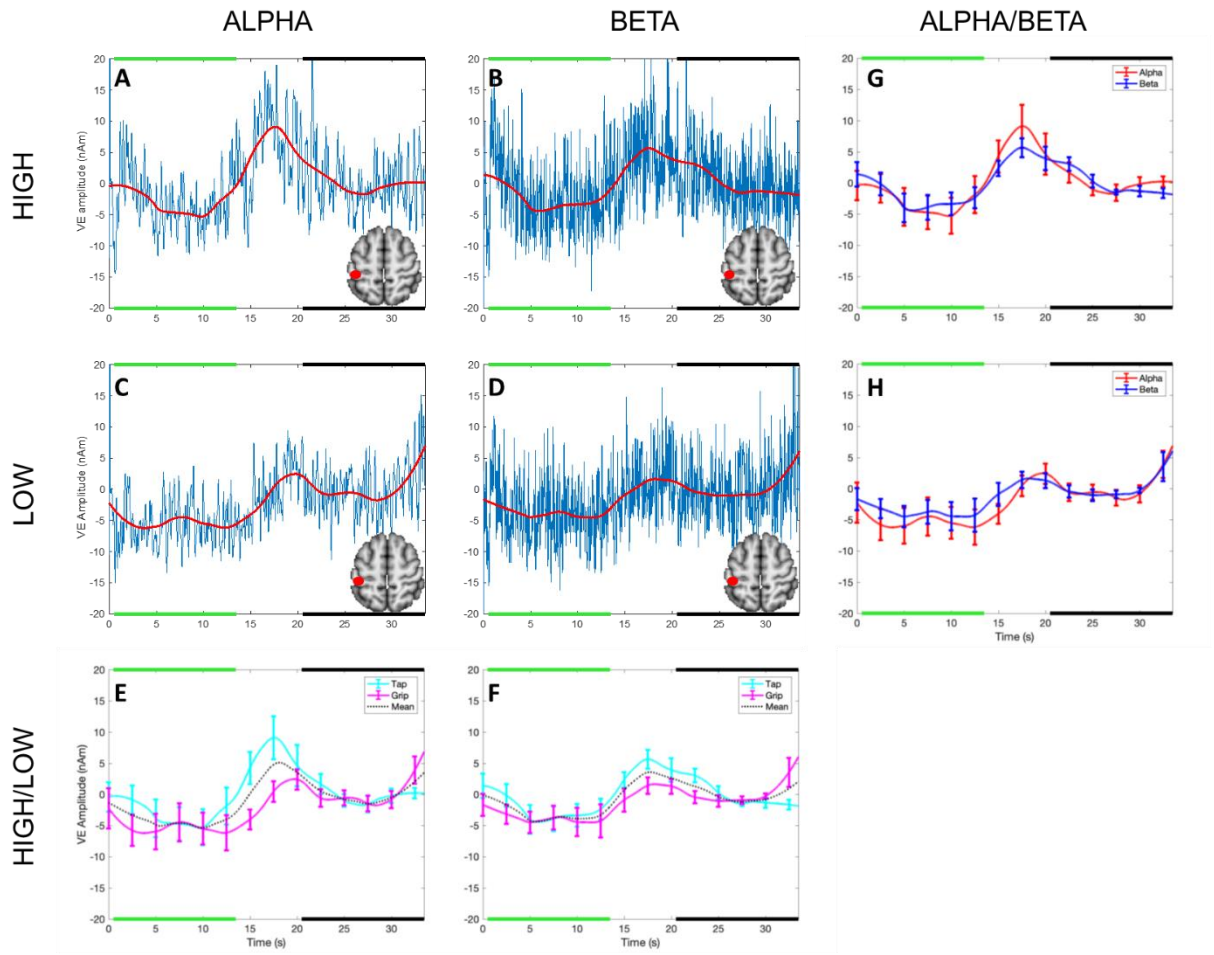

Figure 7. Group average CM visual EEG alpha and beta power timecourses, taken from the mVE.
A and **B** show High alpha and beta group average timecourses respectively (blue= group average raw power timecourse, red=smoothed timecourse). **C** and **D** show Low alpha and beta timecourses respectively. **E** shows the comparison of High and Low alpha responses (cyan/magenta = High/Low smoothed timecourse, respectively); whilst **F** displays the same for beta responses. Error bars denote the standard deviation across subjects. **G** displays the smoothed timecourses of High alpha (red) and beta (blue) responses; whilst **H** shows the same for Low. Stimulus onset at 0 s, 14 s duration (0.5-13.5s used for analysis: green line). Baseline period 20.5-33.5 seconds (black line). Insert of axial brain slices show general region timecourses were extracted from (mVE).

EEG response relationships between frequencies, modalities and stimulus conditions: *Question 2b*

We examined within- and between-subject correlations in EEG response amplitudes to obtain a greater understanding of the relationship of oscillatory responses when

compared between: a) frequency bands, e.g α vs β; b) modalities, e.g. IM vs CM; and c) stimulus conditions (i.e. Tap vs Grip or High vs Low).

a) *Between frequency bands:* Both Grip and Tap data showed significant positive correlations between IM β and IM α (mVE) responses and between CM α and CM β (vVE) responses both within-subject (Table 3B) and across-subjects (Table 3A). Similarly, High and Low contrast data showed significant positive correlations between IM α and IM β (vVE) responses and between CM α and CM β (mVE) responses both within- (Table 4B) and across-subjects (excluding inter-subject High IM α vs IM β which only showed a trend toward significance), Table 4A. These results indicate that single-trial and subject mean responses were highly similar between frequency bands, e.g. that the largest magnitude IM α ERD was associated with the largest magnitude IM β ERD and therefore to simplify subsequent analyses, without compromising functional information, we now focus on the primary oscillation of each modality: visual cortex α and motor cortex β.

b) *Between Modalities:* Across subjects, for both Grip and Tap tasks, significant positive correlations were found between the IM (mVE β) and CM (vVE α) responses (Table 3A). Within subjects, only one subject showed significant positive trial-by-trial IM-CM correlation, no negative correlations were observed (Table 3B). Across subjects in the visual data, significant positive IM-CM correlations were only found for High contrast (IM vVE α vs CM mVE β, Table 4A). Within subjects, only in one subject did the Low contrast data show significant positive trial-by-trial IM-CM correlations, no negative correlations were observed (Table 4B). Therefore for average responses subjects with the strongest IM ERD showed CM ERD to the same stimulus (see Figure S3 for correlation plots that visualise this). No clear within-subject relationship between IM and CM responses was seen when studying trial-by-trial variability. To

determine whether correlations found across subjects were influenced by potential signal leakage between the IM and CM EEG signals, CM EEG power responses were orthogonalised with respect to the IM EEG power (Brookes, Woolrich et al. 2012). For motor trials, CM α power was orthogonalised for each subject across trials with respect to the IM β power, and vice versa for visual trials. Using this data, across subjects, positive correlations between the IM and orthogonalised CM EEG power for motor trials were strengthened (Tap: r=0.61, p<0.05; Grip: r=0.55, p<0.05) while for visual they were unchanged. This suggests the data is unaffected by signal leakage.

c) *Between stimulus conditions.* In the motor data, we found significant positive correlations between subject's mean Grip and Tap IM responses (mVE β) (Table 5). Subject's mean CM responses (vVE α) were also significantly positively correlated between Grip and Tap tasks. In the visual data, only the subject's mean High and Low IM responses (vVE α) were significantly positively correlated (Table 6). No correlation was seen between CM responses (mVE β).

	A		**B**	
	Grip (r, p)	**Tap (r, p)**	**Grip # Subjects**	**Tap # Subjects**
mVE α vs mVE β	.626 <.05	.827 <.001	12/0	14/0
vVE β vs vVE α	.701 <.01	.610 <.05	9/0	8/0
mVE β vs vVE α	.553 <.05	.613 <.05	1/0	2/0

Table 3. Motor trials.
α and β power was extracted from the Motor IM VE (mVE) and Motor CM VE (vVE) during the stimulus period (0.5-13.5s) of Grip and Tap tasks and then correlated across subjects (A) or within subjects between single-trials (B). Rows 1&2 show correlations between frequency bands for IM and CM responses respectively, whilst the 3rd row shows the correlation between IM and CM responses. A) Across-subject IM and CM correlations between α and β power response. B) Number of subjects showing significant positive/negative within-subject correlations (p<0.05) between single-trial responses.

	A		B	
	Low (r, p)	**High (r, p)**	**Low # Subjects**	**High # Subjects**
vVE α vs vVE β	.575 <.05	.359 .19	12/0	12/0
mVE α vs mVE β	.810 <.001	.846 <.001	12/0	13/0
vVE α vs mVE β	.496 .078	.631 <.05	1/0	0/0

Table 4. Visual trials.
α and β power were extracted from the Visual IM VE (vVE) and Visual CM VE (mVE) during the stimulus period (0.5-13.5s) of Low and High stimuli and then correlated across subjects (A) or within subjects between single-trials (B). Rows 1&2 show correlations between frequency bands for IM and CM responses respectively, whilst the 3rd row shows the correlation between IM and CM responses, A) Across-subject IM and CM correlations between α and β power response. The mean power during the stimulus period was baseline corrected and then correlated across subjects. B) Number of subjects showing significant positive/negative within-subject correlations ($p<0.05$) between single-trial responses.

	(r, p)
Grip mVE β vs Tap mVE β	.587 <.05
Grip vVE α vs Tap vVE α	.794 <.001

Table 5. Motor task.
Across-subject correlations between the Tap and Grip response for the Motor IM VE (mVE) β and also the Motor CM VE (vVE) α.

	(r, p)
Low vVE α vs High vVE α	.829 <.001
Low mVE β vs High mVE β	.334 .223

Table 6. Visual task.
across-subject correlations between the High and Low response for the Visual IM VE (vVE) α and Visual CM VE (mVE) β.

Between-subject variability in CM ERD/ERS and corresponding BOLD responses: *Question 3*

We largely found no clear CM α or β ERD/ERS in the group average responses (Figs 5&7) and in addition observed a positive correlation between subjects' CM and IM EEG response amplitudes (Fig S3). Therefore, we investigated between-subject variability in CM EEG responses to further understand the relationship between concurrent responses in the visual and motor cortex. For both visual and motor data subgroups of those subjects showing CM ERD and those showing CM ERS were created, and the mean CM VE response timecourses of those subgroups examined. Beamformer maps from representative subjects displaying CM ERD and ERS for motor and visual data can be seen in Figure 3 E-H.

Motor data

The α power extracted from the vVE during motor tasks showed that the motor CM response varied between ERD and ERS across subjects (Figure 8 A&B). Approximately half the subjects showed CM ERS of vVE α that was sustained throughout motor tasks compared to baseline (Tap, Subjects: 2,6,8,9,10,12,14, mean ERS = 5.8 ± 3.8nAm, Figure 8A; Grip Subjects: 2,6,8,9,10 mean ERS= 7.7 ± 6.4nAm, Figure 8B). The remaining subjects showed sustained CM α ERD during the motor task (Tap Figure 8A: mean ERD = -7.8 ± 8.7nAm; Grip Figure 8B: mean ERD= -9.9 ± 12.8nAm). A greater number of subjects showed CM α ERS during the more complex Tap task than during Grip. A clear separation in vVE power between CM ERS and CM ERD subgroups was observed throughout the duration of the stimulus period. An interesting variation in the shape of the EEG response can be

observed, where peak ERS amplitude was reached in the first half of the stimulation period, particular for the beta responses. It is interesting to note that the “rebound” was still preserved following the ERS, suggesting the occurrence of this response was not necessitated by a preceding ERD and making the description of it as a rebound of oscillatory power seem less appropriate in such circumstances.

Visual data

Similarly, in the visual data we observed a sustained CM β ERS in motor cortex in a subset of subjects (High, Figure 9A, Subjects: 1,5,6,14,15 mean ERS = 3.5± 3.2nAm; Low, Figure 9B, Subjects: 1,2,4,6,13,14 mean ERS = 1.6 ± 1.0nAm), while the remainder showed CM β ERD (High: Figure 9A; mean ERD = -3.4 ± 3.4nAm, Low: Figure 9B; mean ERD = -5.6 ± 5.8nAm). Note the subjects who exhibited CM ERS to motor stimuli were not the same subjects as those who exhibited it for visual stimuli. Similar to the motor data, the post-stimulus rebound appeared for ERS and ERD subjects, despite clear differences in response amplitude during stimulation.

CM EEG vs fMRI relationships

Here we explore whether the presence of a CM ERS or ERD has any corresponding local PBR/NBR signature. In the motor task data, we found no correlation between subject’s CM EEG (vVE α) and BOLD responses in visual cortex (Figure 8C&D). However, in the visual task data we observed a significant negative correlation between subject’s CM EEG (mVE β) and BOLD responses in motor cortex (Figure 9C&D).

To further address this, we performed an additional fixed-effects group level GLM analysis ($Z>2.3$, $p<0.05$ cluster corrected) and compared the mean NBR between

those subjects showing CM ERS and those showing ERD. The number of subjects in each group was balanced by reducing the largest group size by removing the subjects with the weakest EEG responses (closest to zero). For the motor data, the mean CM NBR of the subjects who showed either CM ERS or CM ERD α power from the vVE are plotted in Figure 8E&F for Tap and Grip respectively. Results of a GLM contrast between the ERD and ERS groups are overlaid showing those regions with greater CM NBR (in red) for that specific group. Motor tasks evoked larger mean NBR in visual cortex in the subjects that showed CM ERD than in those subjects that showed CM ERS. Visual trials showed the opposite effect and supported the between-subject visual CM EEG-BOLD correlations (Figure 9C&D). The mean CM NBR for the subjects who showed mVE β CM ERD and separately ERS to visual trials are plotted in Figure 9E&F (High and Low respectively). These plots show that visual stimuli evoked larger mean NBR in motor cortex in the subjects that showed CM ERS than in those who showed CM ERD. These results demonstrate that both the polarity and amplitude of a subject's average CM EEG response was associated with differences in the amplitude of their CM NBR to the same stimulus.

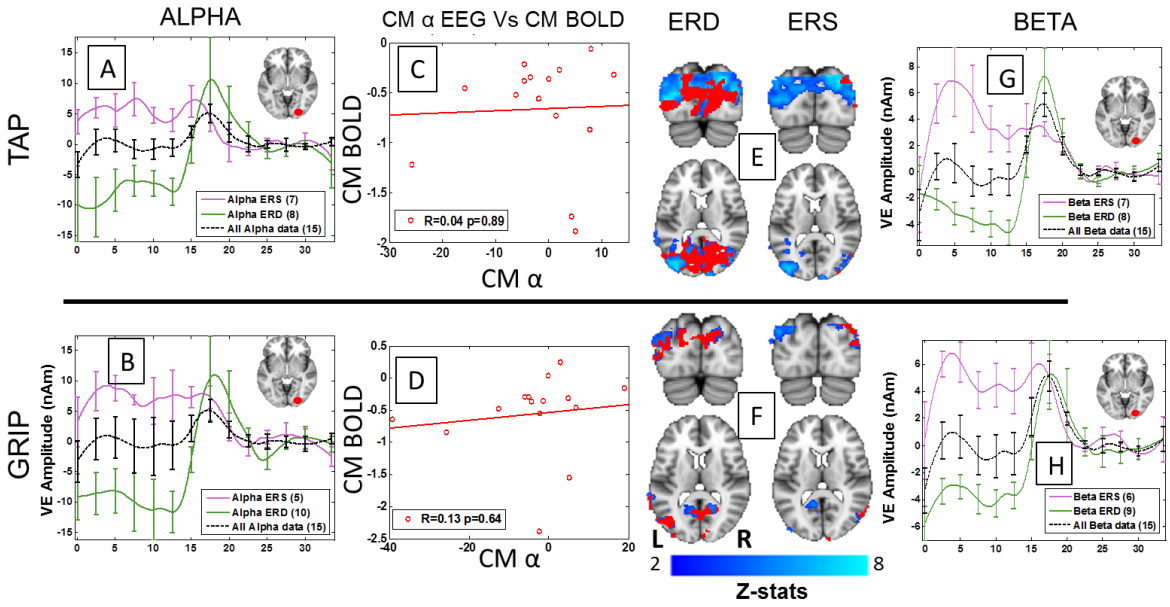

Fig 8. Exploration of CM EEG responses to motor trials.
A and B: subjects were divided into those showing α CM ERS (red) and those showing α CM ERD (blue) with mean subject response (as in Fig 5) in black. Legends show in brackets the number of subjects contributing to each plot. A and B show CM α responses to Tap and Grip respectively. C and D show Pearson's correlations between CM BOLD response and CM alpha power for Tap and Grip respectively, the legend shows the R and p value for the Pearson's correlation. E (Tap) and F (Grip) show the CM NBR (blue) from the group main effect GLM analysis Z>2.3, p<0.05 cluster corrected) for those subjects showing ERD and those showing ERS separately, with significant differences when contrasting one group against the other shown in red (e.g. red in the ERD data shows that the NBR in that region is significantly greater than for the ERS subjects). G and H show those subjects with β CM ERS (red) and those with β CM ERD (blue) with mean subject response (as in Fig 5)

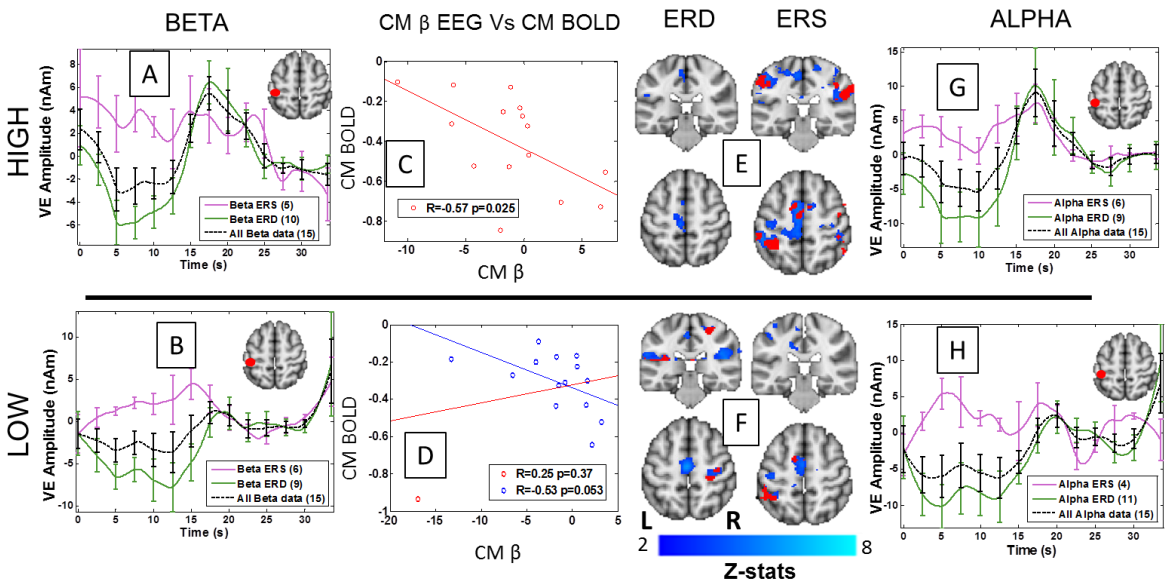

Fig 9. Exploration of CM β EEG responses to visual trials.
For A and B, subjects were divided into those showing β CM ERS (pink) and those showing β CM ERD (green) with mean subject response (as shown in Fig 6) plotted in black, legends show in brackets the number of subjects contributing. A and B show β CM responses to High and Low respectively. C and D show Pearson's correlations between CM BOLD response and CM β power for High and Low respectively, the legend shows the R and p value for the Pearson's correlation. E (High) and F (Low) show the CM NBR (blue) from the group main effect GLM analysis Z>2.3, p<0.05 cluster corrected) for those subjects showing ERD and those showing ERS separately, with significant differences when contrasting one group against the other shown in red (e.g. red in the ERD data shows that the NBR in that region is significantly greater than for the ERS subjects). Additionally, G and H show those subjects with α CM ERS (red) and those with α CM ERD (blue) with mean subject response (as shown in Fig 5)

Single-trial EEG-fMRI Correlations: *Question 3*

The observed positive correlation of EEG response amplitudes suggests that frequency bands (Figures 4-8; Tables 3&4) and task conditions (Tables 5&6) shared a highly comparable response to the stimuli. This enabled concurrent EEG-fMRI single-trial correlation analysis to be conducted for all motor trials together and also for all visual trials together, using regressors formed from β responses in the motor

cortex (IM/CM responses to motor/visual tasks respectively) and α responses in the visual cortex (IM/CM responses to visual/motor tasks respectively).

Motor trials

Intra-modal β mVE-BOLD correlations:

A significant negative correlation was found between the IM β stimulus power and the BOLD response overlapping regions of IM PBR (Figure 10B), indicating that the magnitude of the IM PBR increased as the magnitude of the IM ERD increased. Positive correlations between the IM β stimulus power and the BOLD response were found in areas of the bilateral LOC, IPL and precuneus which overlapped with the CM NBR (Figure 10A), suggesting that with larger magnitude β ERD during motor trials there was larger magnitude CM NBR in the LOC and IPL. This is consistent with the earlier finding when comparing responses between motor conditions (Tap > Grip) that larger IM mVE ERD (Figure 4F) was linked with larger CM NBR in visual cortex (Figure 1), suggesting this cross-modal effect is a general principle of the responses to the motor task. Therefore for stimulus responses to motor tasks we observed correlations between IM EEG and IM PBR as well as IM EEG and CM NBR, with no correlation noted between IM EEG and IM NBR.

Cross-modal α vVE-BOLD correlations:

Significant negative correlations were found between the CM α stimulus power and the BOLD response to motor tasks in regions overlapping with IM PBR, and small regions of CM PBR (Figure 10C&D); suggesting that as IM PBR increased CM ERD

increased. No positive correlations were found between BOLD and the CM α stimulus power.

Visual trials

Intra-modal α vVE-BOLD correlations:

Negative correlations were found between the IM α stimulus power and the IM BOLD response, overlapping regions of main effect PBR mostly located in LOC (Figure 10 E&F), showing that greater IM α ERD during visual trials was associated with larger IM PBR. Positive correlations were observed between IM α vVE stimulus period power and the BOLD response in the left (ipsilateral) LOC during visual trials (Figure 10E), a region of IM NBR during High visual stimuli (Figure 2). This suggests that with greater α ERD at the vVE during visual trials there was a larger NBR in the left LOC.

Cross-modal β mVE-BOLD correlations:

Negative correlations were found between the CM β stimulus power and the IM BOLD response, overlapping regions of visual cortex PBR, suggesting that as IM PBR increased the magnitude of CM ERD increased. Positive β mVE-BOLD correlations were also found in bilateral motor cortex during visual stimuli (Figure 10H; in regions that showed CM NBR in the main effect results). This suggests that visual stimuli that induced higher β power responses in the motor cortex, also showed smaller magnitude NBR and vice versa.

Therefore for stimulus responses to visual tasks we observed a correlation between IM EEG and IM BOLD responses, and between CM EEG and CM BOLD responses, but not between IM EEG and CM BOLD responses.

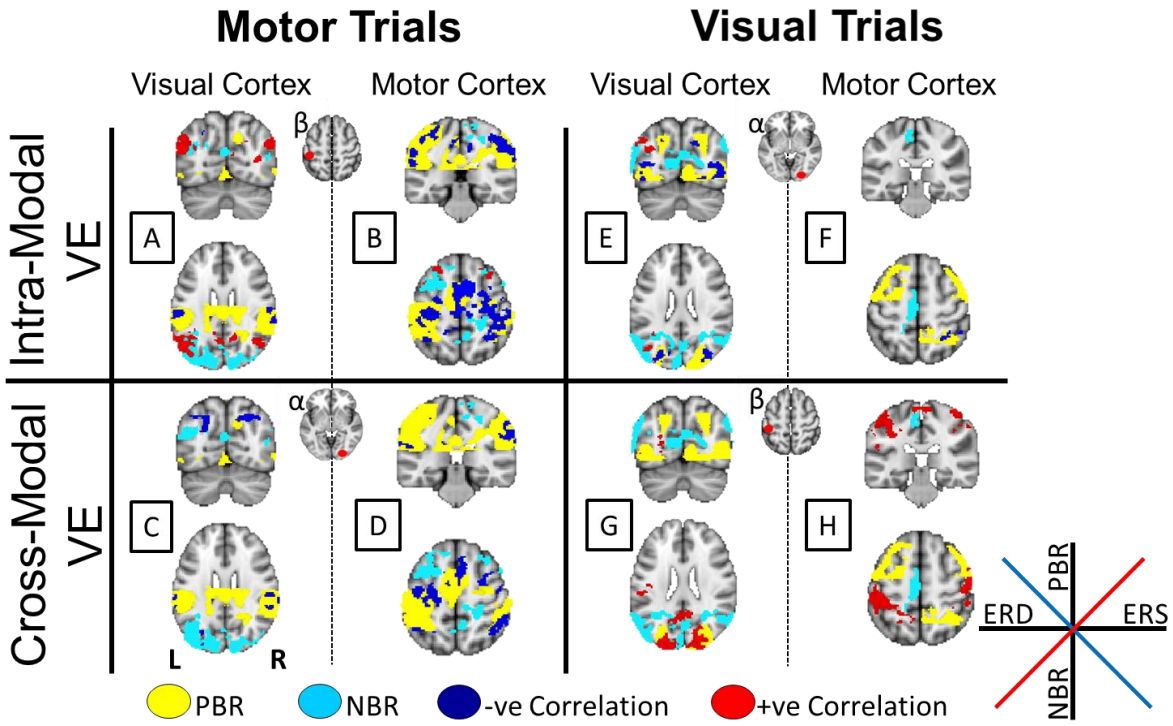

Figure 10. Overlaid main effect (all motor data combined or all visual data combined) and single-trial EEG-BOLD correlations (all significant regions shown). Yellow denotes main effect PBR for all motor trials (**A-D**) and all visual trials (**E-H**). Cyan denotes main effect NBR for all motor trials (**A-D**) and all visual trials (**E-H**). Red shows regions of significant positive EEG-BOLD correlation and blue shows regions of significant negative EEG-BOLD correlation. **A**, **B**, **E** and **F** show correlation maps overlaid onto main effect maps for IM EEG correlations with BOLD responses (β for **A** and **B**; α for **E** and **F**). **C**, **D**, **G** and **H** show correlation maps overlaid onto main effect maps for CM EEG correlations with BOLD responses (α for **C** and **D**; β for **G** and **H**). Visual cortex: y=29, z=48; Motor cortex: y=48, z=63.

Discussion

We used simultaneous EEG-BOLD-CBF recordings to study negative BOLD responses in sensory cortex occurring: within the stimulated modality (IM) ipsilateral

to the stimulation; or in an unstimulated sensory modality (CM). Our aim was to understand the relationship of these two different manifestations of NBRs with underlying CBF and EEG signal changes. We also investigated the relationships between these two types of NBR and between NBR and PBR amplitude/location. To our knowledge this is the first such study of reciprocal visual and motor NBRs using two separate tasks. We discuss the main findings with respect to the three questions initially posed.

1) Cross-modal NBR is elicited by motor and visual stimuli, and both IM and CM NBRs are modulated by task/stimulus intensity

We found that unilateral, single-modality stimuli (volitional motor or passive visual) induced NBRs in unstimulated areas of both motor and visual cortex with overlapping NCBF.

In the current data we observed only a weak effect of stimulus intensity on the IM PBR in the visual or motor data, observing only a ~1% increase in PBR amplitude between 10% and 100% visual contrast and no change for different motor tasks (see also Figure S4). This contrasts with some previous findings (Shmuel, Yacoub et al. 2002), but could be explained by our Tap and Grip motor tasks involving little difference in force output or pacing (Dai, Liu et al. 2001) and that visual flicker rate may be a stronger determinant of response amplitude than contrast (Kwong, Belliveau et al. 1992, Liang, Ances et al. 2013). However, both IM and CM NBR magnitudes increased with stimulus intensity in both visual and motor conditions (Figs 1,2 &S4 and Tables 1&2) replicating and extending previous IM findings

(Shmuel, Yacoub et al. 2002, Klingner, Hasler et al. 2010). In addition, we observed parallels of this effect in the EEG data as, compared to Grip, the Tap motor task induced larger IM ERD, as well as a greater number of subjects with CM ERS of visual cortex α power. However, no differences were observed in the IM EEG responses between High and Low visual stimuli, similar to the PBR result.

2a) There are intrinsic relationships between IM NBRs and CM NBRs

A subject's CM NBR was not related to their IM PBR amplitude (Figure S1), suggesting the level of CM suppression was not simply proportional to the degree of IM sensory activation. However, for the motor tasks the largest IM NBR occurred concurrently with the largest magnitude CM NBR (Figure S2), suggesting a mutual suppression of the two cortical areas not directly required for the task. The lack of coupling between the NBR and PBR suggests that the NBR amplitude is not solely determined by the level of bottom-up stimulus processing and may contain contributions from systems outside of the primary sensory cortex, such as top-down control e.g. from the parietal or frontal cortex (Corbetta and Shulman 2002, Gazzaley, Cooney et al. 2005, Lauritzen, D'Esposito et al. 2009).

2b) There are intrinsic relationships between IM EEG and CM EEG

Fluctuations in the power of alpha oscillations are widely reported to represent temporal variations in cortical excitability (Romei, Brodbeck et al. 2008). Alpha power is commonly decreased (ERD) in sensory cortex during the processing of information, reflecting increased excitation, higher levels of alpha power have been linked to increased cortical inhibition, such as reactive ERS above baseline in sensorimotor or Sternberg tasks (Adrian 1944, Neuper and Pfurtscheller 2001,

Jensen, Gelfand et al. 2002, Neuper, Wörtz et al. 2006), or the more widely studied relative changes between occipital hemispheres due to proactive allocation of spatial attention (Worden, Foxe et al. 2000, Rihs, Michel et al. 2007, Zumer, Scheeringa et al. 2014). Fluctuations in IM alpha power have been closely linked to both PBR and NBR amplitudes during passive visual stimulation (Mayhew, Ostwald et al. 2013). Here, we investigated whether such findings extend between sensory cortices using tasks involving minimal attentional demands.

The EEG data showed a further example of the positive relationship between IM and CM responses seen in the NBR data. Consistently across both modalities and conditions a positive correlation of between-subject variability in IM and CM EEG response amplitudes was observed (Figure S3). Subjects who showed a CM ERD also showed the strongest magnitude IM ERD (i.e. most negative EEG amplitude) to the same stimulus; and subjects that showed a CM ERS also showed the weakest magnitude IM ERD. Such positive coupling between visual and motor cortex EEG responses was seen in all tasks, a consistency which suggests this reflects a fundamental property of the brain's response.

This positive IM-CM EEG coupling appears counter-intuitive as a negative correlation where greater activation (ERD) of the stimulated/IM cortex is associated with greater suppression (ERS) of the CM sensory modality could be expected, as previously reported in fMRI within a single modality (Shmuel, Yacoub et al. 2002, Klingner, Hasler et al. 2010). However, along with the lack of a relationship between IM PBR and CM NBR, both our EEG and fMRI data suggest that in terms of average responses this simple case of stronger activation concurrent with stronger deactivation was not found for either task. Taken together with our other findings,

that CM NBR was unrelated to IM PBR, these results partly support previous findings (Hairston, Hodges et al. 2008, Mozolic, Joyner et al. 2008), in suggesting that CM NBR reflects the level of suppression of a non-stimulated (CM) modality, whilst not clearly evidencing that processing is prioritised within the stimulated (IM) modality, potentially due to the absence of a sufficiently demanding task which requires strong downregulating of sources of sensory interference.

3) ***IM and CM NBR are related to IM and CM EEG responses therefore providing evidence for a neuronal origin***

IM NBRs were consistently accompanied by a significant IM ERD in α/β oscillations. In contrast, despite the group showing CM NBR on average, subjects were divided between those showing CM ERS and ERD. We report no clear group-level CM EEG response and found α and β CM ERS in a subset of subjects (between 27% and 46%) depending upon the task and frequency band (Figs. 8A&B and 9A&B). Surprisingly, CM ERS responses during the stimulus period were seen inconsistently both within- and between-subjects for a single modality (e.g. subject 4 showed CM β ERS during Low but CM β ERD during High), while other subjects showed consistent α and β CM ERS in a single modality (e.g. subject 2 shows α and β CM ERS during Grip and Tap) (Figs. 5 and 7). ERS responses have been previously measured in the motor cortex to visual stimulation (Koshino and Niedermeyer 1975, Pfurtscheller 1992) and vice versa (Neuper and Pfurtscheller 2001)also with a lack of consistency across individuals, e.g. only seen in 54% of subjects (Koshino and Niedermeyer 1975)

Importantly, we found that the between subject variability in CM ERS/ERD was related to individual subjects CM NBR amplitude, with a negative coupling between ERS and NBR shown by two separate analyses of the visual data (Fig 9). Furthermore, EEG-fMRI correlations between trial-by-trial variability of α/β power and both IM and CM NBR magnitude (Fig 10) add to evidence for a relationship, albeit complex, between NBRs and neuronal activity. Together these results highlight that IM and CM NBRs are related to local changes in neuronal activity. However, given the between subjects correlation we observed between IM ERD and the CM EEG response (see Tables 3&4 and Figure S3), caution should be exercised when definitively attributing differences in fMRI response to CM response polarity, rather than IM responses.

In contrast to the mean responses, trial-by-trial EEG-fMRI analysis showed that a coupling of larger IM activation with larger CM deactivation occurred at the single-trial level in the motor data (Figure 10). We have shown in previous work that single-trial response correlations occur with opposite polarity to that shown in the average responses (Mayhew, Mullinger et al. 2016). This finding suggests that the dynamic temporal evolution of responses contains the anticipated functional relationship of collaborating IM activation and CM suppression. No equivalent relationship between CM NBR and IM α ERD was observed in the visual dataset, although IM PBRs were found to correlate with IM and CM EEG responses (Figure 10E&G respectively). This represents the second instance (in addition to IM-CM NBR, Figure S2) where cross-modal coupling is observed only in the motor task, we believe this arises due to a difference in the brains processing of the two tasks related to their differing demands. The passive nature of the visual stimuli induced more automatic, bottom-up sensory responses compared to the volitional, active performance of the motor

task, good performance of which requires greater task engagement and top-down attentional control. We suggest that this top-down control exerts influence over the lower level sensory systems to optimise task performance and drives greater collaboration between the two sensory systems during Tap and Grip than during visual stimulation (Corbetta and Shulman 2002, Ciaramitaro, Burač as et al. 2007). Trial-by-trial EEG-fMRI correlations provides further evidence that IM and CM NBRs are related to changes in neuronal activity. CM NBR showed a significant positive correlation with mVE β power, where the CM NBR amplitude increased as motor cortex β power increased.

Bilateral IM ERD of both α and β power, strongest contralaterally, were consistently measured across subjects during both motor tasks and visual stimuli (Figs. 4 and 7), whilst, in contrast, a clear lateralisation of contralateral positive and ipsilateral negative IM BOLD and CBF responses was observed as previously reported (Allison, Meador et al. 2000, Mullinger, Mayhew et al. 2014). IM NBR have been previously shown to correlate negatively with IM α power during median nerve stimulation (Mullinger, Mayhew et al. 2014), but the current study found no links between IM NBR and α/β using different tasks. Therefore the source of this discrepancy between EEG and fMRI response polarities remains unresolved, however it is likely that the stronger contralateral α and β ERD are associated with the widely reported contralateral gamma ERS (Muthukumaraswamy 2010) and tentative reports suggest a gamma ERD occurring ipsilateral to finger movements (Huo, Xiang et al. 2010) would appear a plausible correlate of ipsilateral NBR in line with rodent work (Boorman, Kennerley et al. 2010, Boorman, Harris et al. 2015). A few previous studies have measured gamma EEG responses using sparse fMRI sequences (Mulert, Leicht et al. 2010, Scheeringa, Fries et al. 2011), including a

recent demonstration that gamma ERS during motor abductions is positively correlated with IM motor PBR (Uji, Wilson et al. 2018), however the implementation of the DABS sequence employed here was not designed to be used in that manner.

Between-subject relationships of CM ERS and NBR

Our hypothesis that CM ERS would be observed over CM NBR regions, reflecting a neural measure of the suppression of processing in the unstimulated system, was not consistently shown across our group containing ERS and ERD subjects. The ERS had an inherently smaller response amplitude than the ERD (compare Figures 4&6 with 8&9). Therefore, this lack of a consistent CM ERS either reflects: a lack of measurement sensitivity, a limitation of EEG source analysis (as discussed in: Potential limitations) or an overt replacement by the ERD response. It also suggests that the CM ERS was a less automatic process than the consistently observed IM bilateral ERD. Overall we found a relationship between CM ERS and CM NBR, but the direction of this relationship was dependent upon the exact task conditions. A negative relationship was seen in the visual data, where subject's with stronger mean CM ERS showed greater magnitude CM NBR in motor cortex, providing persuasive evidence of a link between the two responses. This negative coupling was not replicated in the motor data, a result that could partially arise from subject's fixation on the visually displayed motor cue, thus creating a visual ERD which counteracts any CM ERS effect elicited by the motor task performance. However, as CM ERD occurred in response to both tasks, the presence of the visual cue in the motor paradigm cannot explain this effect. Instead we suggest that the CM ERD reflects differences in arousal and cortical excitability whereby in some subjects

desynchronization of low frequency oscillations was more widespread across multiple cortical networks than in others, perhaps indicating an inefficiency of network segregation in some subjects and a reduced ability to suppress activity in task-irrelevant sensory systems. The possibility must also be considered that due to the simple tasks employed the demand to inhibit task-irrelevant cortex may not have been sufficient to induce CM ERS in all subjects. A consequent implication being that CM NBR arises from additional mechanisms, including neural activity at frequencies beyond the alpha/beta bends studied here.

It is interesting to note that the motor CM ERS responses display a relatively large increase in power in the first half of the stimulus period followed by a lower but still elevated level of power (Figure 8 G&H). This perhaps arises due to the long duration of the stimuli (14s) and subjects not maintaining a consistent level of engagement after task initialisation. This observation may suggest that the ERS is a naturally more transient, less sustained response than the ERD.

Potential limitations of methodology and comparison between EEG recorded inside and outside the MRI scanner

Visual stimulation induced CM NBR and negative CBF with a high degree of spatial agreement to the IM motor contralateral PBR (Figure 2) and the IM ERD (mVE). In comparison, motor stimulation induced a slightly more complex pattern of CM BOLD responses, with CM NBR in anterior and bilateral LOC and a CM PBR in small bilateral regions of posterior visual cortex. We suggest this pattern could arise from either visual imagery of the motor movement (as the subject's hand was at their

sides and out of sight in the scanner) or focussing on the visual word cue instructing the task performance. The relatively long duration of the stimulus period (14s) means that we would expect the visual cue to contribute little BOLD response, with it primarily generated at cue onset and offset rather than during the whole stimulation period. The presence of both CM NBR and PBR within the visual cortex complicates the understanding of the origin of the CM α response; although, as shown by the group beamformer maps, the location of the vVE lies in dorsal visual areas approximating the LOC (Figure 3), closer to the CM NBR observed in superior occipital cortex.

As we study visual and motor cortex responses to an interleaved paradigm of visual and motor tasks there is the possibility that some carry-over effects may have occurred to influence signals in nonstimulated (but in this context relevant) cortex. We do not think it significantly present in this data for several reasons. Firstly because we used a baseline interval of 20s which is longer than most fMRI studies and generally considered long enough to allow recording independent stimulus responses. Secondly, previous work using visual and somatosensory tasks found no impact of a pre-existing negative BOLD response on the peak response amplitude of a subsequent positive BOLD response (Refs), suggesting that even small residual effects in our data would not cause large response modulations.

It cannot be ruled out that an explanation that the observed positive coupling of IM and CM EEG responses (Fig S3) arises from limitations of the LCMV beamformer and EEG volume conduction that may impair our ability to distinctly separate activity from sources in the visual and motor cortices. For instance, due to possible inaccuracies in the headmodels or imperfections in the solution of the inverse

problem it is possible that signal leakage from the stronger IM source confounds measurement of the CM response, a situation that would be exacerbated in a subject with naturally high levels of occipital alpha power who showed a widespread ERD that extended over parietal cortex and into anterior sensorimotor regions. By correcting for signal leakage we have shown that there is little/no change in the correlations between IM and CM EEG power across subjects, therefore highlighting our ability to distinguish the signals using the VEs defined. Additionally, our observation that IM β and CM α responses correlate differently with the BOLD signal suggests they reflect different sensory signals and aren't driven by signal leakage.

Due to MRI gradient and ballistocardiogram artefacts inherent in recording EEG-simultaneously with fMRI the reliability of our ability to measure CM ERS signals in the lower signal-to-noise MR environment could be questioned. To provide a comparative assessment of the reliability of the EEG recordings inside the scanner and to familiarise the subjects with the stimuli, EEG recordings of responses to Tap and High conditions only were collected outside of the scanner whilst subject's sat upright in front of a computer monitor that displayed the same visual stimulation and motor cues as during scanning. Twenty-two trials were recorded for each of the conditions, 14/14s stimulus/baseline (active period: 0.5-10.5s; passive period: 17.5-27.5s). EEG data were analysed as described for data recorded inside the scanner, and motor and visual cortex CM responses extracted from the IM VE locations as defined from the scanner data. Figure S5 shows that we observed patterns of α and β CM ERS during stimulation that were highly similar to those seen in the inside scanner data. On average, Tap induced no CM response whereas High induced a weak CM ERD. On further inspection it was found that subjects were again divided between those showing ERS and those showing ERD (Motor Tap: α, ERS subjects:

1,3,4,5,7,10,12,14; mean = 5.1± 5.5nAm; Visual High: β, ERS subjects: 1,3,4,9 mean = 3.4 ± 3.4nAm). This suggests that our observations inside the scanner are not confounded by the MR environment artefacts, or movements occurring inside the magnetic field, but reflect neuronal activity related to the stimuli.

Conclusion

This work supports the hypothesis that IM NBRs are at least partially neuronal in origin and further shows this to also be the case for CM NBRs, with IM as well as CM NBRs modulated by stimulus intensity.

References

Adrian, E. D. (1944). "Brain rhythms." Nature **153**: 360-362.
Allen, P. J., O. Josephs and R. Turner (2000). "A method for removing imaging artifact from continuous EEG recorded during functional MRI." Neuroimage **12**(2): 230-239.
Allison, J. D., K. J. Meador, D. W. Loring, R. E. Figueroa and J. C. Wright (2000). "Functional MRI cerebral activation and deactivation during finger movement." Neurology **54**(1): 135-142.
Amedi, A., R. Malach and A. Pascual-Leone (2005). "Negative BOLD differentiates visual imagery and perception." Neuron **48**(5): 859-872.
Bianciardi, M., M. Fukunaga, P. van Gelderen, J. A. de Zwart and J. H. Duyn (2011). "Negative BOLD-fMRI signals in large cerebral veins." J Cereb Blood Flow Metab **31**(2): 401-412.
Boorman, L., S. Harris, M. Bruyns-Haylett, A. Kennerley, Y. Zheng, C. Martin, M. Jones, P. Redgrave and J. Berwick (2015). "Long-latency reductions in gamma power predict hemodynamic changes that underlie the negative BOLD signal." J Neurosci **35**(11): 4641-4656.
Boorman, L., A. J. Kennerley, D. Johnston, M. Jones, Y. Zheng, P. Redgrave and J. Berwick (2010). "Negative blood oxygen level dependence in the rat: a model for investigating the role of suppression in neurovascular coupling." J Neurosci **30**(12): 4285-4294.
Bright, M. G., M. Bianciardi, J. A. de Zwart, K. Murphy and J. H. Duyn (2014). "Early anti-correlated BOLD signal changes of physiologic origin." Neuroimage **87**: 287-296.
Brinkman, L., A. Stolk, H. C. Dijkerman, F. P. de Lange and I. Toni (2014). "Distinct roles for alpha- and beta-band oscillations during mental simulation of goal-directed actions." J Neurosci **34**(44): 14783-14792.
Brinkman, L., A. Stolk, T. R. Marshall, S. Esterer, P. Sharp, H. C. Dijkerman, F. P. de Lange and I. Toni (2016). "Independent Causal Contributions of Alpha- and Beta-Band Oscillations during Movement Selection." J Neurosci **36**(33): 8726-8733.
Brookes, M. J., K. J. Mullinger, C. M. Stevenson, P. G. Morris and R. Bowtell (2008). "Simultaneous EEG source localisation and artifact rejection during concurrent fMRI by means of spatial filtering." Neuroimage **40**(3): 1090-1104.
Brookes, M. J., M. W. Woolrich and G. R. Barnes (2012). "Measuring functional connectivity in MEG: A multivariate approach insensitive to linear source leakage." Neuroimage **63**(2): 910-920.
Buckner, R. L., J. R. Andrews-Hanna and D. L. Schacter (2008). "The brain's default network: anatomy, function, and relevance to disease." Ann N Y Acad Sci **1124**: 1-38.
Carlqvist, H., V. V. Nikulin, J. O. Stromberg and T. Brismar (2005). "Amplitude and phase relationship between alpha and beta oscillations in the human electroencephalogram." Med Biol Eng Comput **43**(5): 599-607.
Ciaramitaro, V. M., G. T. Buračas and G. M. Boynton (2007). "Spatial and Cross-Modal Attention Alter Responses to Unattended Sensory Information in Early Visual and Auditory Human Cortex." Journal of Neurophysiology **98**(4): 2399-2413.
Ciaramitaro, V. M., H. M. Chow and L. G. Eglington (2017). "Cross-modal attention influences auditory contrast sensitivity: Decreasing visual load improves auditory thresholds for amplitude- and frequency-modulated sounds." J Vis **17**(3): 20.
Corbetta, M. and G. L. Shulman (2002). "Control of goal-directed and stimulus-driven attention in the brain." Nat Rev Neurosci **3**(3): 201-215.

Dai, T. H., J. Z. Liu, V. Sahgal, R. W. Brown and G. H. Yue (2001). "Relationship between muscle output and functional MRI-measured brain activation." Exp Brain Res **140**(3): 290-300.
Desikan, R. S., F. Ségonne, B. Fischl, B. T. Quinn, B. C. Dickerson, D. Blacker, R. L. Buckner, A. M. Dale, R. P. Maguire, B. T. Hyman, M. S. Albert and R. J. Killiany (2006). "An automated labeling system for subdividing the human cerebral cortex on MRI scans into gyral based regions of interest." NeuroImage **31**(3): 968-980.
Devor, A., P. Tian, N. Nishimura, I. C. Teng, E. M. C. Hillman, S. N. Narayanan, I. Ulbert, D. A. Boas, D. Kleinfeld and A. M. Dale (2007). "Suppressed neuronal activity and concurrent arteriolar vasoconstriction may explain negative blood oxygenation level-dependent signal." J Neurosci **27**(16): 4452-4459.
Foxe, J. J. and A. C. Snyder (2011). "The Role of Alpha-Band Brain Oscillations as a Sensory Suppression Mechanism during Selective Attention." Front Psychol **2**: 154.
Fu, K. M., J. J. Foxe, M. M. Murray, B. A. Higgins, D. C. Javitt and C. E. Schroeder (2001). "Attention-dependent suppression of distracter visual input can be cross-modally cued as indexed by anticipatory parieto-occipital alpha-band oscillations." Brain Res Cogn Brain Res **12**(1): 145-152.
Garcia, D. M., G. Duhamel and D. C. Alsop (2005). "Efficiency of inversion pulses for background suppressed arterial spin labeling." Magnetic Resonance in Medicine **54**(2): 366-372.
Gazzaley, A., J. W. Cooney, K. McEvoy, R. T. Knight and M. D'Esposito (2005). "Top-down enhancement and suppression of the magnitude and speed of neural activity." J Cogn Neurosci **17**(3): 507-517.
Glover, G. H., T. Q. Li and D. Ress (2000). "Image-based method for retrospective correction of physiological motion effects in fMRI: RETROICOR." Magn Reson Med **44**(1): 162-167.
Haegens, S., L. Luther and O. Jensen (2012). "Somatosensory anticipatory alpha activity increases to suppress distracting input." J Cogn Neurosci **24**(3): 677-685.
Hairston, W. D., D. A. Hodges, R. Casanova, S. Hayasaka, R. Kraft, J. A. Maldjian and J. H. Burdette (2008). "Closing the mind's eye: deactivation of visual cortex related to auditory task difficulty." Neuroreport **19**(2): 151-154.
Harel, N., S.-P. Lee, T. Nagaoka, D.-S. Kim and S.-G. Kim (2002). "Origin of negative blood oxygenation level-dependent fMRI signals." J Cereb Blood Flow Metab **22**(8): 908-917.
Heeger, D. J., A. C. Huk, W. S. Geisler and D. G. Albrecht (2000). "Spikes versus BOLD: what does neuroimaging tell us about neuronal activity." Nat Neurosci **3**: 631-633.
Huber, L., J. Goense, A. J. Kennerley, D. Ivanov, S. N. Krieger, J. Lepsien, R. Trampel, R. Turner and H. E. Moller (2014). "Investigation of the neurovascular coupling in positive and negative BOLD responses in human brain at 7 T." Neuroimage **97**: 349-362.
Huo, X., J. Xiang, Y. Wang, E. G. Kirtman, R. Kotecha, H. Fujiwara, N. Hemasilpin, D. F. Rose and T. Degrauw (2010). "Gamma oscillations in the primary motor cortex studied with MEG." Brain Dev **32**(8): 619-624.
Jenkinson, M., P. Bannister, M. Brady and S. Smith (2002). "Improved optimization for the robust and accurate linear registration and motion correction of brain images." Neuroimage **17**(2): 825-841.
Jenkinson, M. and S. Smith (2001). "A global optimisation method for robust affine registration of brain images." Med Image Anal **5**(2): 143-156.
Jensen, O., J. Gelfand, J. Kounios and J. E. Lisman (2002). "Oscillations in the alpha band (9-12 Hz) increase with memory load during retention in a short-term memory task." Cereb Cortex **12**(8): 877-882.
Jerbi, K., J. R. Vidal, T. Ossandon, S. S. Dalal, J. Jung, D. Hoffmann, L. Minotti, O. Bertrand, P. Kahane and J.-P. Lachaux (2010). "Exploring the electrophysiological correlates

of the default-mode network with intracerebral EEG." Frontiers in systems neuroscience **4**: 27-27.
Kannurpatti, S. S. and B. B. Biswal (2004). "Negative functional response to sensory stimulation and its origins." J Cereb Blood Flow Metab **24**(6): 703-712.
Kastrup, A., J. Baudewig, S. Schnaudigel, R. Huonker, L. Becker, J. M. Sohns, P. Dechent, C. Klingner and O. W. Witte (2008). "Behavioral correlates of negative BOLD signal changes in the primary somatosensory cortex." Neuroimage **41**(4): 1364-1371.
Klimesch, W., P. Sauseng and S. Hanslmayr (2007). "EEG alpha oscillations: the inhibition-timing hypothesis." Brain Res Rev **53**(1): 63-88.
Klingner, C. M., K. Ebenau, C. Hasler, S. Brodoehl, Y. Görlich and O. W. Witte (2011). "Influences of negative BOLD responses on positive BOLD responses." Neuroimage.
Klingner, C. M., C. Hasler, S. Brodoehl and O. W. Witte (2010). "Dependence of the negative BOLD response on somatosensory stimulus intensity." Neuroimage **53**(1): 189-195.
Klingner, C. M., G. F. Volk, C. Flatz, S. Brodoehl, M. Dieterich, O. W. Witte and O. Guntinas-Lichius (2013). "Components of vestibular cortical function." Behav Brain Res **236**(1): 194-199.
Kobayashi, E., A. P. Bagshaw, C. Grova, F. Dubeau and J. Gotman (2006). "Negative BOLD responses to epileptic spikes." Hum Brain Mapp **27**(6): 488-497.
Koshino, Y. and E. Niedermeyer (1975). "Enhancement of Rolandic mu-rhythm by pattern vision." Electroencephalography and Clinical Neurophysiology **38**(5): 535-538.
Kuhtz-Buschbeck, J. P., C. Mahnkopf, C. Holzknecht, H. Siebner, S. Ulmer and O. Jansen (2003). "Effector-independent representations of simple and complex imagined finger movements: a combined fMRI and TMS study." Eur J Neurosci **18**(12): 3375-3387.
Kwong, K. K., J. W. Belliveau, D. A. Chesler, I. E. Goldberg, R. M. Weisskoff, B. P. Poncelet, D. N. Kennedy, B. E. Hoppel, M. S. Cohen and R. Turner (1992). "Dynamic magnetic resonance imaging of human brain activity during primary sensory stimulation." Proc Natl Acad Sci U S A **89**(12): 5675-5679.
Laurienti, P. J., J. H. Burdette, M. T. Wallace, Y. F. Yen, A. S. Field and B. E. Stein (2002). "Deactivation of sensory-specific cortex by cross-modal stimuli." J Cogn Neurosci **14**(3): 420-429.
Lauritzen, T. Z., M. D'Esposito, D. J. Heeger and M. A. Silver (2009). "Top-down flow of visual spatial attention signals from parietal to occipital cortex." J Vis **9**(13): 18 11-14.
Liang, C. L., B. M. Ances, J. E. Perthen, F. Moradi, J. Liau, G. T. Buracas, S. R. Hopkins and R. B. Buxton (2013). "Luminance contrast of a visual stimulus modulates the BOLD response more than the cerebral blood flow response in the human brain." Neuroimage **64**: 104-111.
Logothetis, N. K., J. Pauls, M. Augath, T. Trinath and A. Oeltermann (2001). "Neurophysiological investigation of the basis of the fMRI signal." Nature **412**(6843): 150-157.
Maggioni, E., E. Molteni, C. Zucca, G. Reni, S. Cerutti, F. M. Triulzi, F. Arrigoni and A. M. Bianchi (2015). "Investigation of negative BOLD responses in human brain through NIRS technique. A visual stimulation study." NeuroImage **108**: 410-422.
Mandelkow, H., P. Halder, P. Boesiger and D. Brandeis (2006). "Synchronization facilitates removal of MRI artefacts from concurrent EEG recordings and increases usable bandwidth." Neuroimage **32**(3): 1120-1126.
Mayhew, S. D., K. J. Mullinger, D. Ostwald, C. Porcaro, R. Bowtell, A. P. Bagshaw and S. T. Francis (2016). "Global signal modulation of single-trial fMRI response variability: Effect on positive vs negative BOLD response relationship." Neuroimage **133**: 62-74.

Mayhew, S. D., D. Ostwald, C. Porcaro and A. P. Bagshaw (2013). "Spontaneous EEG alpha oscillation interacts with positive and negative BOLD responses in the visual-auditory cortices and default-mode network." Neuroimage **76**: 362-372.
Mazaheri, A. and O. Jensen (2010). "Shaping Functional Architecture by Oscillatory Alpha Activity: Gating by Inhibition." Frontiers in Human Neuroscience **4**(4): 186.
McKiernan, K. A., J. N. Kaufman, J. Kucera-Thompson and J. R. Binder (2003). "A parametric manipulation of factors affecting task-induced deactivation in functional neuroimaging." J Cogn Neurosci **15**(3): 394-408.
Mozolic, J. L., D. Joyner, C. E. Hugenschmidt, A. M. Peiffer, R. A. Kraft, J. A. Maldjian and P. J. Laurienti (2008). "Cross-modal deactivations during modality-specific selective attention." BMC Neurol **8**: 35.
Mulert, C., G. Leicht, P. Hepp, V. Kirsch, S. Karch, O. Pogarell, M. Reiser, U. Hegerl, L. Jager, H. J. Moller and R. W. McCarley (2010). "Single-trial coupling of the gamma-band response and the corresponding BOLD signal." Neuroimage **49**(3): 2238-2247.
Mullinger, K. J. and R. Bowtell (2011). "Combining EEG and FMRI." Methods in molecular biology (Clifton, N.J.) **711**: 303-326.
Mullinger, K. J., M. T. Cherukara, R. B. Buxton, S. T. Francis and S. D. Mayhew (2017). "Post-stimulus fMRI and EEG responses: Evidence for a neuronal origin hypothesised to be inhibitory." NeuroImage **157**: 388-399.
Mullinger, K. J., S. D. Mayhew, A. P. Bagshaw, R. Bowtell and S. T. Francis (2014). "Evidence that the negative BOLD response is neuronal in origin: a simultaneous EEG-BOLD-CBF study in humans." Neuroimage **94**: 263-274.
Mullinger, K. J., P. S. Morgan and R. W. Bowtell (2008). "Improved artifact correction for combined electroencephalography/functional MRI by means of synchronization and use of vectorcardiogram recordings." J Magn Reson Imaging **27**(3): 607-616.
Muthukumaraswamy, S. D. (2010). "Functional properties of human primary motor cortex gamma oscillations." J Neurophysiol **104**(5): 2873-2885.
Neuper, C. and G. Pfurtscheller (2001). "Event-related dynamics of cortical rhythms: frequency-specific features and functional correlates." Int J Psychophysiol **43**(1): 41-58.
Neuper, C., M. Wörtz and G. Pfurtscheller (2006). "ERD/ERS patterns reflecting sensorimotor activation and deactivation." Prog Brain Res **159**: 211-222.
Olman, C. A., S. Inati and D. J. Heeger (2007). "The effect of large veins on spatial localization with GE BOLD at 3 T: Displacement, not blurring." Neuroimage **34**(3): 1126-1135.
Oostenveld, R., P. Fries, E. Maris and J. M. Schoffelen (2011). "FieldTrip: Open source software for advanced analysis of MEG, EEG, and invasive electrophysiological data." Comput Intell Neurosci **2011**: 156869.
Pasley, B. N., B. A. Inglis and R. D. Freeman (2007). "Analysis of oxygen metabolism implies a neural origin for the negative BOLD response in human visual cortex." Neuroimage **36**(2): 269-276.
Pfurtscheller, G. (1992). "Event-related synchronization (ERS): an electrophysiological correlate of cortical areas at rest." Electroencephalogr Clin Neurophysiol **83**(1): 62-69.
Pfurtscheller, G. and F. H. Lopes da Silva (2005). "EEG event-related desynchronisation (ERD) and event-related synchronisation." Electroencephalography: Basic Principles, Clinical Applications and Related Fields **Lippincott Williams and Wilkins, Philadephia.**(Niedermeyer, E., Lopes da Silva, F. (Eds)): 1003-1016.
Pfurtscheller, G., C. Neuper and W. Mohl (1994). "Event-related desynchronization (ERD) during visual processing." Int J Psychophysiol **16**(2-3): 147-153.

Pfurtscheller, G., A. Stancak, Jr. and C. Neuper (1996). "Event-related synchronization (ERS) in the alpha band--an electrophysiological correlate of cortical idling: a review." Int J Psychophysiol **24**(1-2): 39-46.
Puckett, A. M., J. R. Mathis and E. A. DeYoe (2014). "An investigation of positive and inverted hemodynamic response functions across multiple visual areas." Hum Brain Mapp **35**(11): 5550-5564.
Rihs, T. A., C. M. Michel and G. Thut (2007). "Mechanisms of selective inhibition in visual spatial attention are indexed by alpha-band EEG synchronization." Eur J Neurosci **25**(2): 603-610.
Ritter, P., M. Moosmann and A. Villringer (2009). "Rolandic alpha and beta EEG rhythms' strengths are inversely related to fMRI-BOLD signal in primary somatosensory and motor cortex." Hum Brain Mapp **30**(4): 1168-1187.
Robinson, S. E. and J. Vrba (1999). "Functional neuroimaging by synthetic aperture magnetometry (SAM)." Recent Advances in Biomagnetism **Tohoku University Press, Sendai**: 302-305.
Romei, V., V. Brodbeck, C. Michel, A. Amedi, A. Pascual-Leone and G. Thut (2008). "Spontaneous fluctuations in posterior alpha-band EEG activity reflect variability in excitability of human visual areas." Cereb Cortex **18**(9): 2010-2018.
Schafer, K., F. Blankenburg, R. Kupers, J. M. Gruner, I. Law, M. Lauritzen and H. B. Larsson (2012). "Negative BOLD signal changes in ipsilateral primary somatosensory cortex are associated with perfusion decreases and behavioral evidence for functional inhibition." Neuroimage **59**(4): 3119-3127.
Scheeringa, R., P. Fries, K.-M. Petersson, R. Oostenveld, I. Grothe, D. G. Norris, P. Hagoort and M. C. M. Bastiaansen (2011). "Neuronal Dynamics Underlying High- and Low-Frequency EEG Oscillations Contribute Independently to the Human BOLD Signal." Neuron **69**(3): 572-583.
Schridde, U., M. Khubchandani, J. E. Motelow, B. G. Sanganahalli, F. Hyder and H. Blumenfeld (2008). "Negative BOLD with large increases in neuronal activity." Cereb Cortex **18**(8): 1814-1827.
Shmuel, A., M. Augath, A. Oeltermann and N. K. Logothetis (2006). "Negative functional MRI response correlates with decreases in neuronal activity in monkey visual area V1." Nat Neurosci **9**(4): 569-577.
Shmuel, A., E. Yacoub, J. Pfeuffer, P. F. Van de Moortele, G. Adriany, X. Hu and K. Ugurbil (2002). "Sustained negative BOLD, blood flow and oxygen consumption response and its coupling to the positive response in the human brain." Neuron **36**(6): 1195-1210.
Singh, M., S. Kim and T.-S. Kim (2003). "Correlation between BOLD-fMRI and EEG signal changes in response to visual stimulus frequency in humans." Magn Reson Med **49**(1): 108-114.
Sten, S., K. Lundengard, S. T. Witt, G. Cedersund, F. Elinder and M. Engstrom (2017). "Neural inhibition can explain negative BOLD responses: A mechanistic modelling and fMRI study." Neuroimage **158**: 219-231.
Tal, Z., R. Geva and A. Amedi (2017). "Positive and Negative Somatotopic BOLD Responses in Contralateral Versus Ipsilateral Penfield Homunculus." Cerebral cortex (New York, N.Y. : 1991) **27**(2): 962-980.
Thut, G., A. Nietzel, S. A. Brandt and A. Pascual-Leone (2006). "Alpha-band electroencephalographic activity over occipital cortex indexes visuospatial attention bias and predicts visual target detection." J Neurosci **26**(37): 9494-9502.
Uji, M., R. Wilson, S. T. Francis, K. J. Mullinger and S. D. Mayhew (2018). "Exploring the advantages of multiband fMRI with simultaneous EEG to investigate coupling between

gamma frequency neural activity and the BOLD response in humans." Hum Brain Mapp **39**(4): 1673-1687.
Van Veen, B. D., Van Drongelen, W., Yuchtman, M., Suzuki, A. (1997). "Localisation of brain electrical activity via linearly constrained minimum variance spatial filtering." IEEE Transactions on biomedical engineering **44**(9).
Woolrich, M. W., T. E. Behrens, C. F. Beckmann, M. Jenkinson and S. M. Smith (2004). "Multilevel linear modelling for FMRI group analysis using Bayesian inference." Neuroimage **21**(4): 1732-1747.
Worden, M. S., J. J. Foxe, N. Wang and G. V. Simpson (2000). "Anticipatory biasing of visuospatial attention indexed by retinotopically specific alpha-band electroencephalography increases over occipital cortex." J Neurosci **20**(6): RC63.
Yuan, H., T. Liu, R. Szarkowski, C. Rios, J. Ashe and B. He (2010). "Negative covariation between task-related responses in alpha/beta-band activity and BOLD in human sensorimotor cortex: an EEG and fMRI study of motor imagery and movements." Neuroimage **49**(3): 2596-2606.
Yuan, H., C. Perdoni, L. Yang and B. He (2011). "Differential electrophysiological coupling for positive and negative BOLD responses during unilateral hand movements." J Neurosci **31**(26): 9585-9593.
Zumer, J. M., R. Scheeringa, J. M. Schoffelen, D. G. Norris and O. Jensen (2014). "Occipital alpha activity during stimulus processing gates the information flow to object-selective cortex." PLoS Biol **12**(10): e1001965.

Supplementary Figures

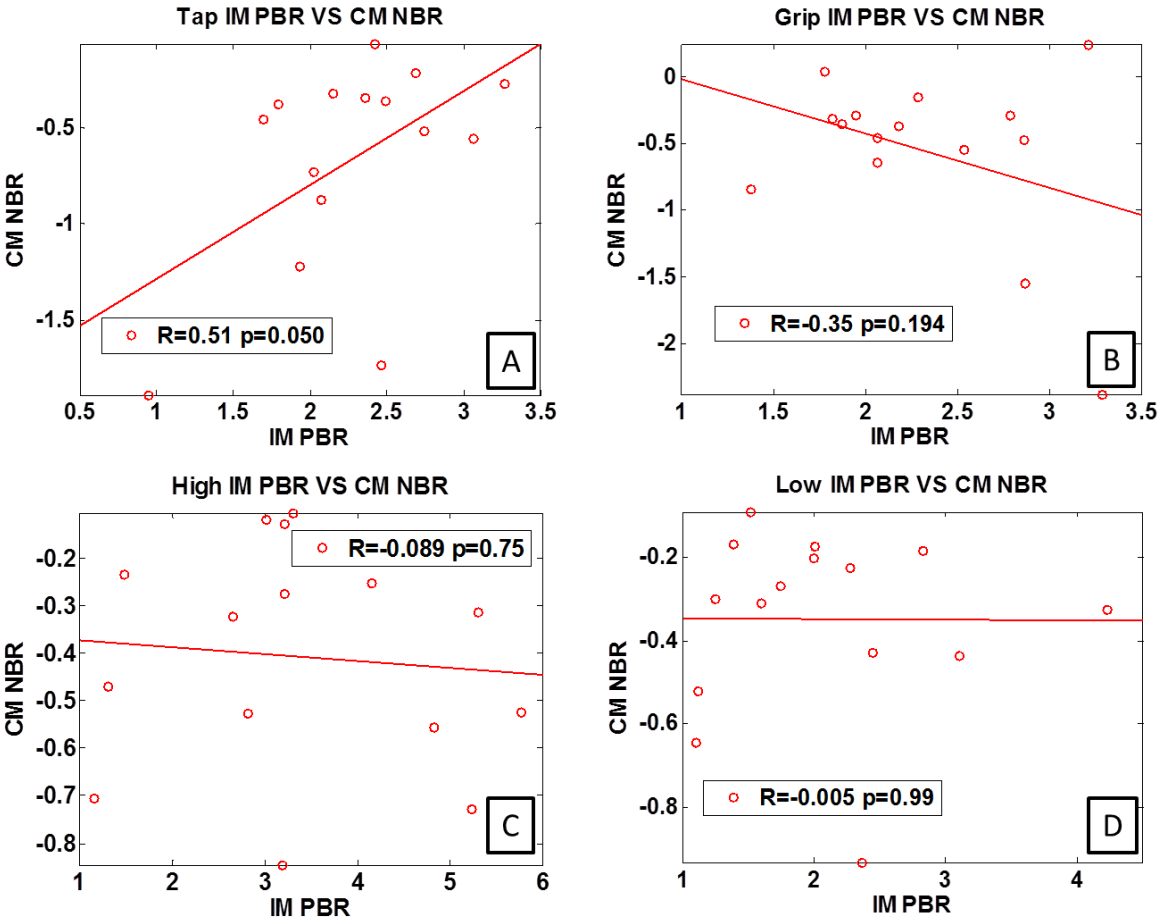

Figure S1. Across subject Pearson's correlations between IM PBR and CM NBR.
A and **B** show IM PBR:CM NBR correlations for Tap and Grip respectively. While no significant correlations were found, Tap exhibits a positive correlation trend. **C** and **D** show IM PBR:CM NBR correlations for High and Low respectively with no significant correlations found.

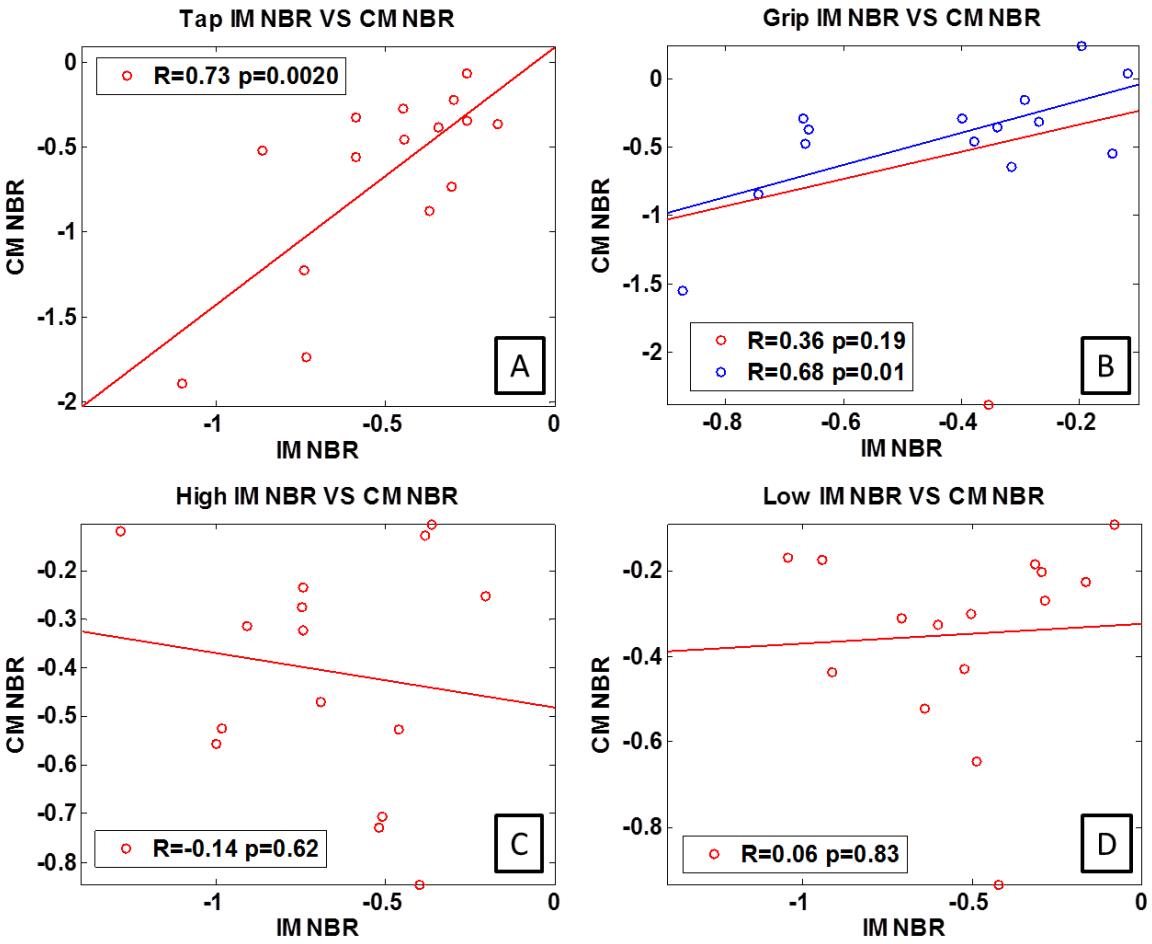

Figure S2. Across subject Pearson's correlations between IM NBR and CM NBR.
A and **B** show IM NBR:CM NBR correlations for Tap and Grip correlations respectively. With a significant positive correlation noted for Tap. For Grip, a significant positive correlation was found after removal of an outlier (red line – all data, blue=without outlier). **C** and **D** show IM NBR:CM NBR correlations for High and Low respectively with no significant correlations found.

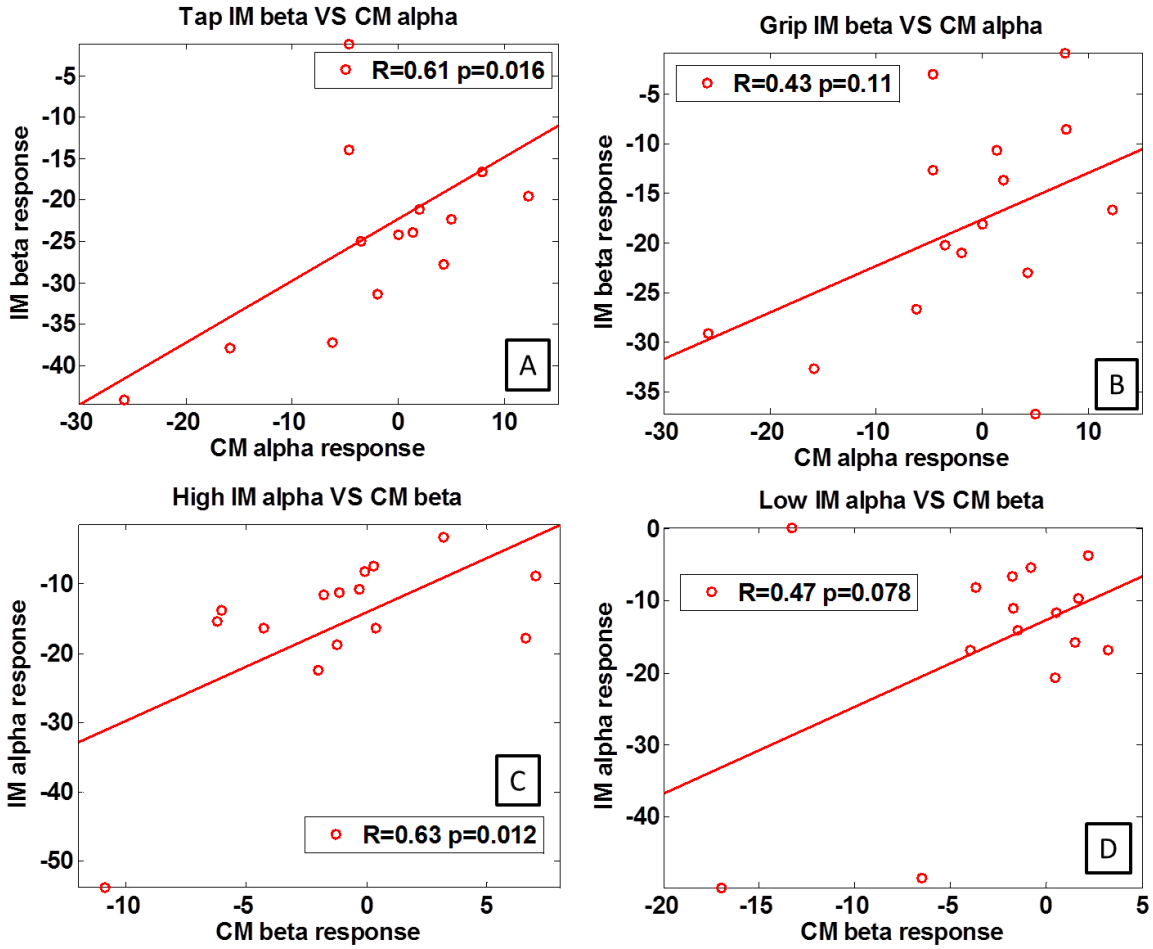

Figure S3. Across subject Pearson's correlations between IM and CM EEG responses.
A and **B** show correlations between IM EEG beta responses and CM EEG alpha responses for Tap and Grip respectively. Tap shows a significant positive correlation while grip exhibits a positive trend. **C** and **D** show correlations between IM EEG alpha responses and CM EEG beta responses for High and Low respectively. Similar to the motor tasks, the more intense stimulus (High) exhibits a significant positive correlation while the less intense stimulus (Low) shows a non-significant positive trend. These positive correlations show that stronger IM ERD is related to CM ERD, while weaker IM ERD is associated with CM ERS.

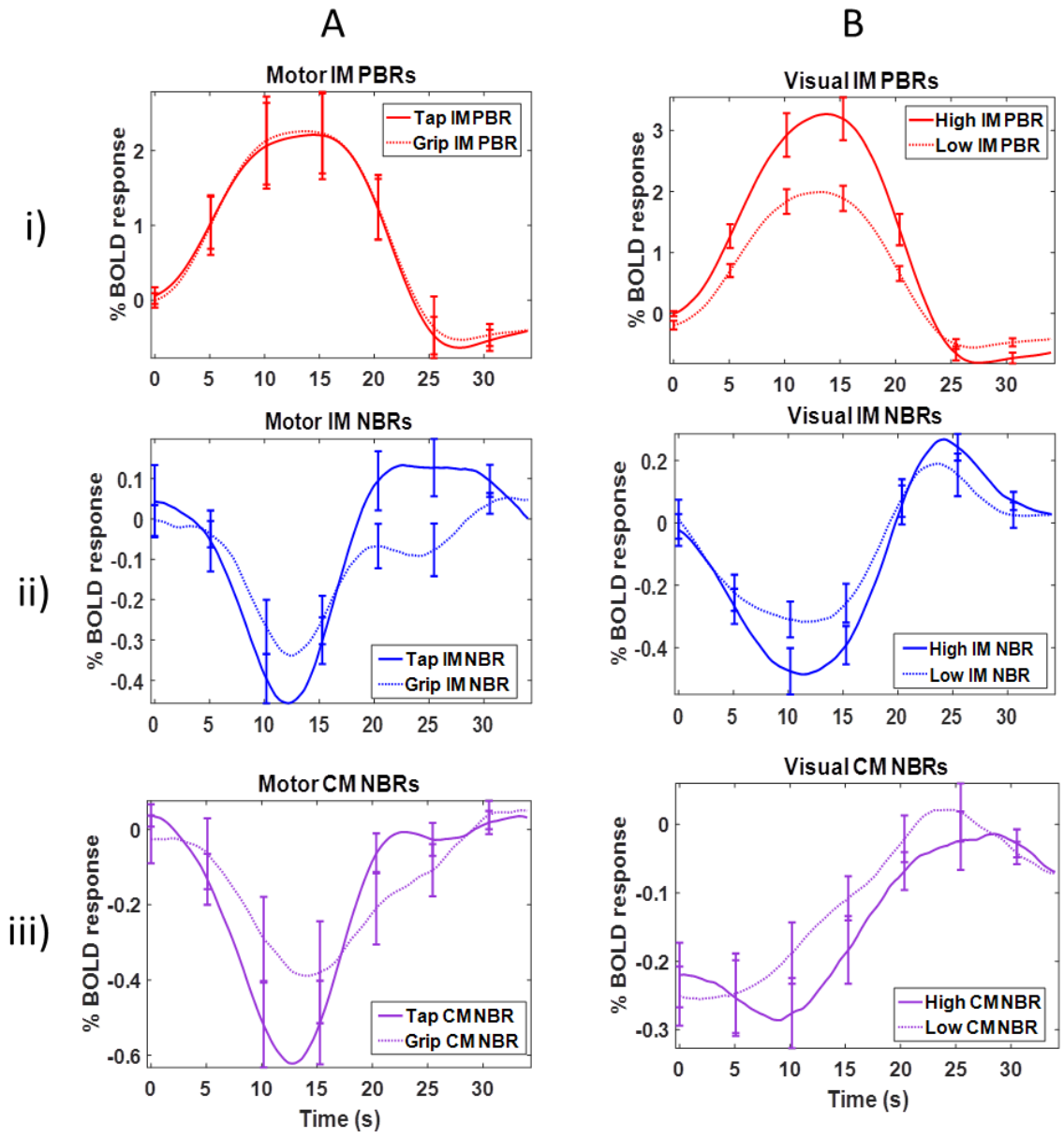

Figure S4. Comparison plots of BOLD response taken from ROIs centred over peak responses in IM/CM masks to each individual task.
A shows motor Tap (solid line) and Grip (dotted line) BOLD responses. **Ai** shows IM PBRs which show little difference in percentage change in BOLD response. Larger IM (**Aii**) and CM (**Aiii**) NBRs were found to Tap task than Grip task.
B shows High (solid line) and Low (dotted line) BOLD responses. **Bi** shows IM PBRs which show that High trials evoked a larger percentage change in BOLD response. Larger IM (**Bii**) and CM (**Biii**) NBRs were found to High than Low.

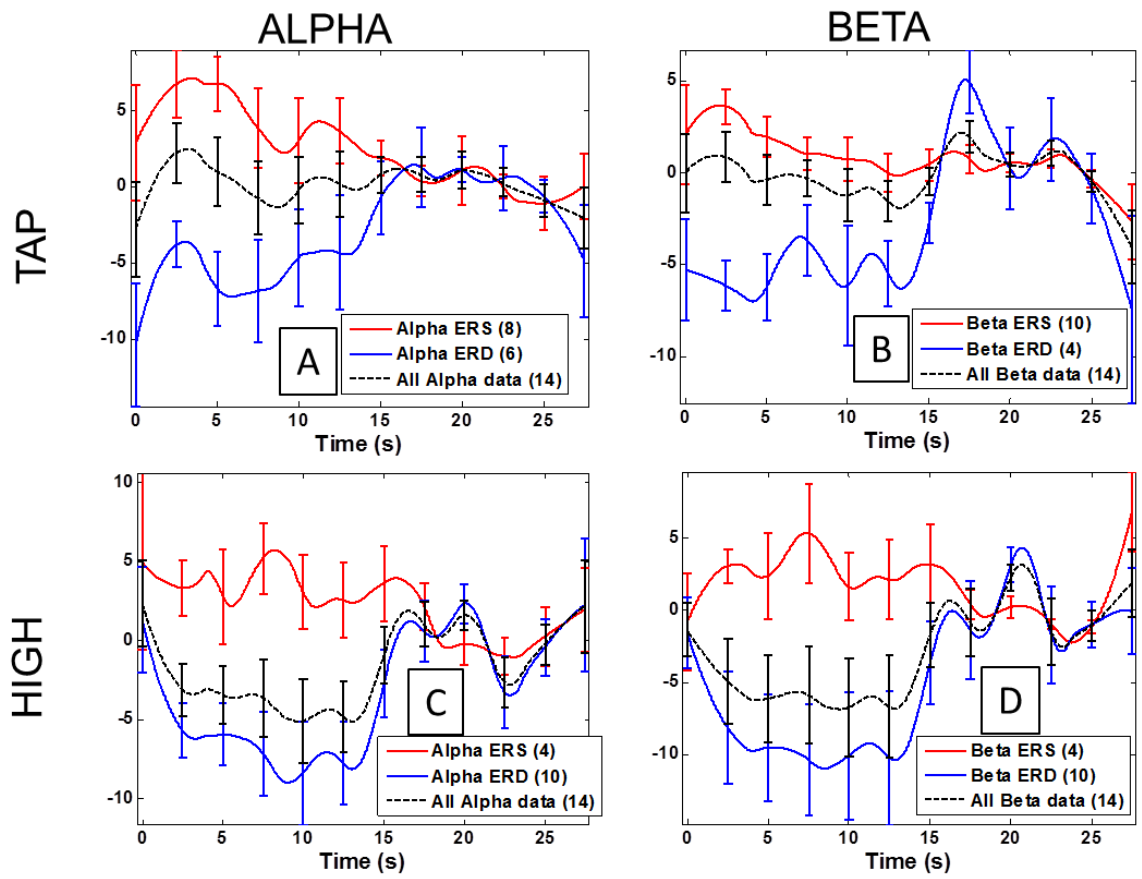

Figure S5. CM EEG responses taken from data collected outside of the scanner prior to the main experiment (n=14).
VE positions were the same as those derived from the main data. Subjects were split into those showing CM ERS and those showing CM ERD and smoothed average timecourses plotted: blue = ERD subjects group average smoothed timecourse; red = ERR subjects group average smoothed timecourse; black = all subjects group smoothed timecourse. **A** and **B** show Tap alpha and beta group average smoothed timecourses respectively. **C** and **D** show High alpha and beta group average smoothed timecourses respectively.